

The Warm Ionized Medium (WIM)

①

Discussed so far:

- Very hot, very tenuous gas ($T \gtrsim 10^6 \text{ K}$); shock ionization by SNR
- Warm gas ($T \sim 10^4 \text{ K}$) @ moderate density, radiatively ionized by stars & clusters

Kulkarni & Heiles (1987)
Interstellar processes

Reynolds (1993) Back to the Galaxy

Haffner, Reynolds, & Tufte (1999)
ApJ 523, 223

Heiles (2000), Fourth Tetow conf.

Haffner et al. (2009) Rev Mod Phys

WIM \triangleq DIG "diffuse ionized gas"

- Source of ionization:
- 1) escaping ^{ionizing} radiation from H II regions, along lines of sight with $\tau_{\text{UV}} \lesssim 1$
 - 2) part of the gas may be partially ionized by X-rays + CRs, partly neutral.

This view of "two WIMs" is argued by Heiles.

The understanding of the IIM is evolving, and this is a subject of research. IT may change ~~over time~~ with time.

Tracers:
→ pulsar dispersion
→ diffuse H α emission

Temp → from $[NII]/H\alpha$ ratio

ionization → $[SII]/[NII]$

$$\frac{I_{6583}}{H\alpha} = 1.63 \times 10^5 \left(\frac{H^+}{H}\right)^{-1} \left(\frac{N}{H}\right) \left(\frac{N^+}{N}\right)$$

$T_4^{0.426} e^{-2.18/T_4}$

WIM

UV absorption against high lat. stars can probe ne, Te on "representative" lines of sight (fairly local)

Dispersion measure observation

Arrival time of pulses changes with frequency as a function of the integrated value of n_e (i.e. the medium is dispersive).

$$\frac{d\omega}{dk} = v_{group} = c \left(1 - \frac{\omega_p^2}{\omega^2}\right)^{1/2} \quad \omega_p^2 = \frac{4\pi n_e e^2}{m_e}$$

(R-L B-17)

2 π plasma frequency ν_p
 $\omega_p = 5.636 \times 10^4 n_e^{1/2} \text{ s}^{-1}$

Then, $\Delta t(\nu)_{arrival} = \frac{e^2}{2\pi m_e c \nu^2} \int_0^d n_e ds$

$\Rightarrow DM \triangleq \int_0^d n_e ds,$

$\Delta t(\nu) = \frac{DM}{241.0 \left(\frac{\nu}{\text{GHz}}\right)^2}$

$[DM] = \text{cm}^{-3} \text{pc}$

Observations of DM to pulsars within 2 kpc of the sun yields

$\langle n_e \rangle = \frac{0.025}{\text{cm}^{-3}} + \frac{0.015}{\text{cm}^{-3}} e^{-|z|/70 \text{pc}}$

"diffuse" comp. from H II regions with scale-height $\sim 1 \text{ kpc}$ (Taylor & Cordes 1993)

Lyne, Manchester, & Taylor (1985)

This is from DM to distant high-lat pulsars in globular clusters

$\langle n_e \rangle_{diffuse} = 0.025 e^{-|z|/\text{kpc}}$

Close to Gal. Center, DM is extremely large, enough to prevent detection of pulsars due to the distortion of their wave form (diff. Fourier components arrive @ different times).

Emission measure H α observation

3

Galactic H α emission $\begin{cases} \rightarrow \text{individual HII regions} \\ \rightarrow \text{diffuse component} \end{cases}$

Diffuse comp. discovered in 70s-80s by R.J. Reynolds (Wisc.)

Sometimes referred to as the "Reynolds layer"

WHAM - "Wisconsin H α ~~receptor~~ Mapper"

Hoffner (2000); Reynolds, Hoffner, & Tuftte (1999)

Since H α is produced by recomb. ; $I_{H\alpha} = \frac{\int n_e^2 ds}{2.75 T_4^{0.9}}$

$$[I] = \text{Rayleighs} = \frac{10^6}{4\pi} \text{ photons cm}^{-2}$$

$$\Rightarrow EM \equiv \int n_e^2 ds \quad \text{"emission measure"}$$

Scale height is determined from fits to several latitudes,

Hoffner et al. find $\sim 1 \text{ kpc}$

Using EM + DM toward pulsars in GCs., we obtain a measure of clumping and volume density

$n_e \sim 0.08 \text{ cm}^{-3}$ with volume filling factor ~ 0.2

$$EM/DM = 0.08 \text{ cm}^{-3}$$

Reynolds (1993)

Reynolds (1991)

ApJ 372, L1

WIM

The underlying assumption is:

4

$$m_e = m_0 + \int m \quad \langle \delta m \rangle = 0 \quad \frac{\langle \delta m^2 \rangle}{m_0^2} = \sigma^2$$
$$\langle EM \rangle = \int (m_0 + \delta m)^2 ds = \int m_0^2 + 2m_0 \delta m + (\delta m)^2 ds$$
$$= m_0^2 (1 + \sigma^2) \cdot L, \quad \text{~~etc~~}$$

$$DM = \int (m_0 + \delta m) ds = m_0 \cdot L$$

$$\Rightarrow \frac{EM}{DM} = \frac{m_0^2 (1 + \sigma^2) L}{m_0 L} = m_0 (1 + \sigma^2)$$

$$\Rightarrow m_0 = \frac{EM/DM}{1 + \sigma^2} \xrightarrow{\sigma \rightarrow 0} EM/DM$$

This assumes a single component. More on this soon.

Temperature: from $[NII]/H\alpha$ ratio

Hoffner, Reynolds & Tufté (1999) find $T \sim 6000 - 10000$ K with 7,000 K as "typical"

T correlated with $n_e^2 \Rightarrow T \uparrow \leftrightarrow n_e^2 \downarrow$, meaning $T \uparrow$ for $z \uparrow$ suggesting a variation in the heating source with height. This is a matter of research.

Heat source;

As in HII, we can compute the energy balance.

Power required for observed $H\alpha$ intensity: 5×10^6 H ionizations $s^{-1} cm^{-2}$,
or 10^{-4} erg $s^{-1} cm^{-2}$ in the plane of the MW. WIM

Assuming ~~1~~ 1 SN every 30 yrs., SN power is $\sim 10^4$ erg $s^{-1} cm^{-2}$

\Rightarrow would require $\sim 100\%$ efficiency to explain $H\alpha$!

There is more power available from O stars:

O stars in the galaxy yields $\sim 3 \times 10^7$ ion. photons $s^{-1} cm^{-2}$

\Rightarrow need $\frac{1}{6}$ of this to escape HII regions to explain $I_{diffuse}(H\alpha)$ (Mathis 1986, APT 301, 423). B stars may also contribute, but much less.

~~Hot gas~~ "leaky" HII regions are easier to explain if hot gas fills much of the galaxy. Heiles (2000) discusses evidence for this in Eridanus superbubble.

Multi component WIM?

From a combination of DM, EM, and UV obs. obs. Heiles suggests that there are two WIM components.

Basic argument: pressure balance. With one entirely ionized component, WIM pressure \ll CNM pressure

$$\frac{P_i}{k} = 2T_i EM/DM \quad EM/DM = 0.08 cm^{-3} \\ = 1100 K cm^{-3}, \text{ about 4 times lower than ONM}$$

If fluctuations $\&$ σ^2 included, this gets worse as

$$\langle n_e \rangle = \frac{EM/DM}{1 + \sigma^2} \Rightarrow \frac{P_i}{k} \text{ could be as low as } 500 K cm^{-3}$$

Heile's solution is to argue that most of EM comes from a partially-ionized (ie, low n_e^2) gas, whereas most of DM comes from fully ionized gas \Rightarrow he shows that this makes pressure more consistent with equilibrium. WIM

What is this partially-ionized component?

⑥

Heiles suggest that it comes from partially-ionized WNM, this is predicted to occur in the McKee-Ostriker model for X-rays and CR penetrating into the WNM. It remains to be proven.

at the

UR

s

des an
distrib-
medium,
e basic
those
atures
solar
rate is
xtend-
out $\frac{1}{8}$
, e.g.,
of ion-
, e.g.,
re av-
e-half

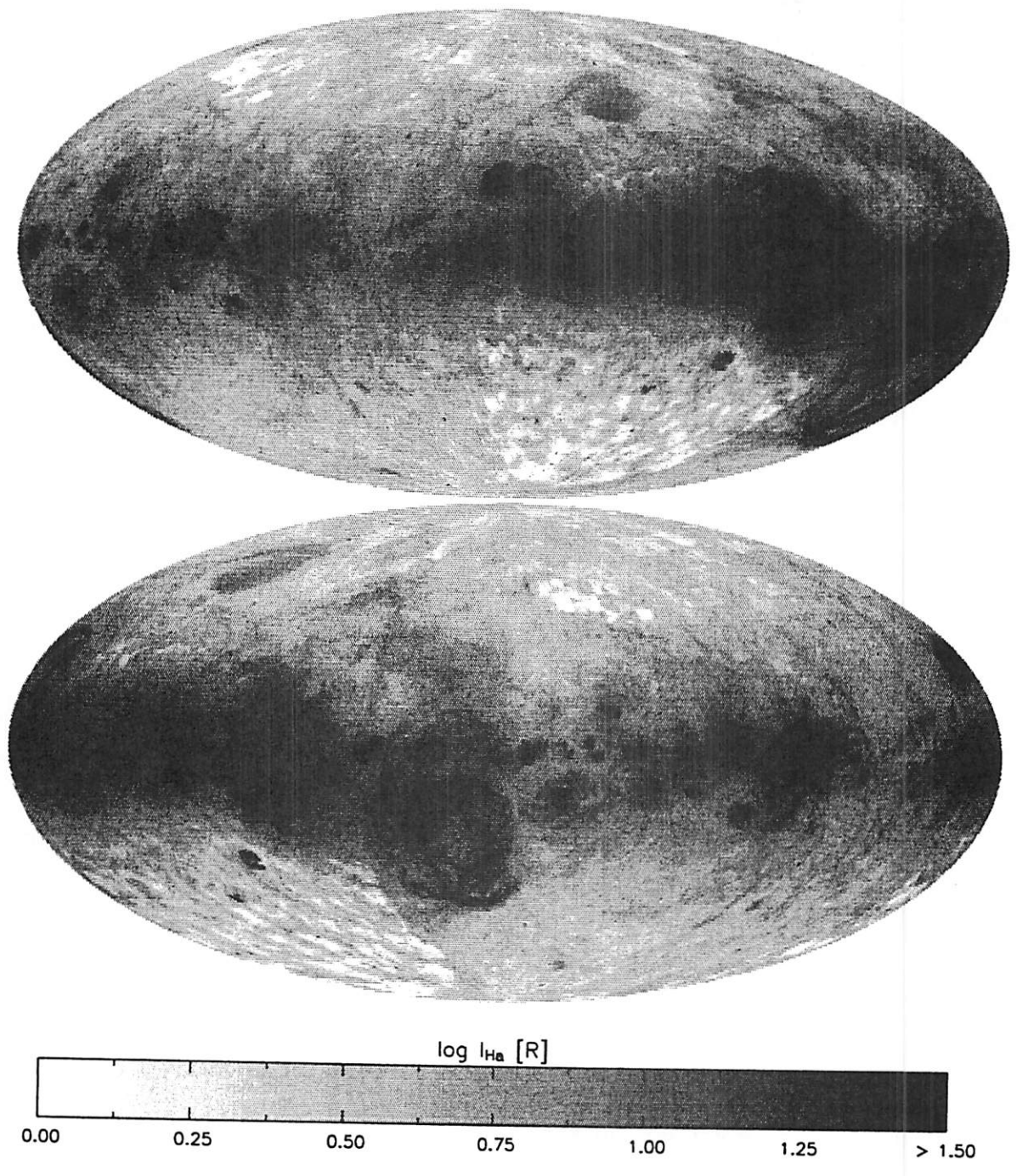
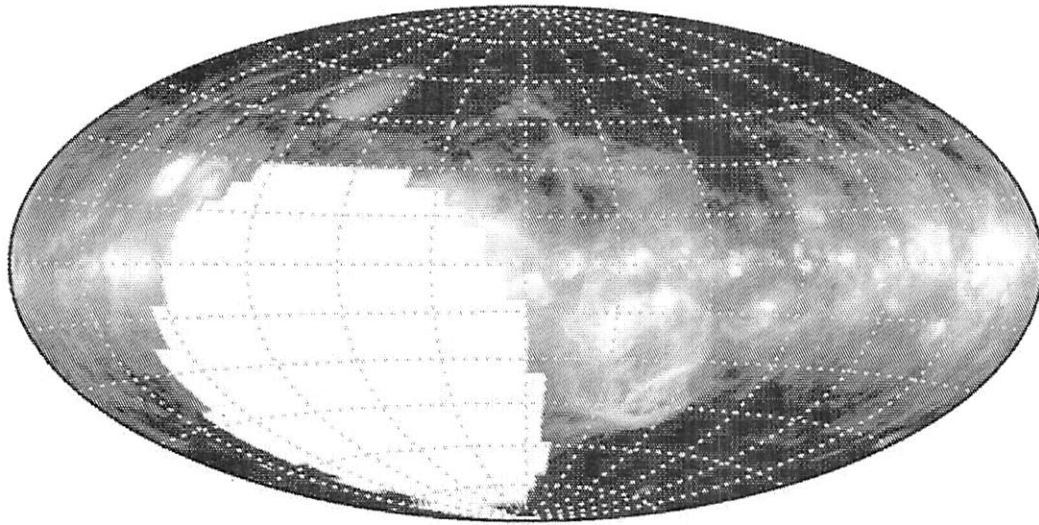
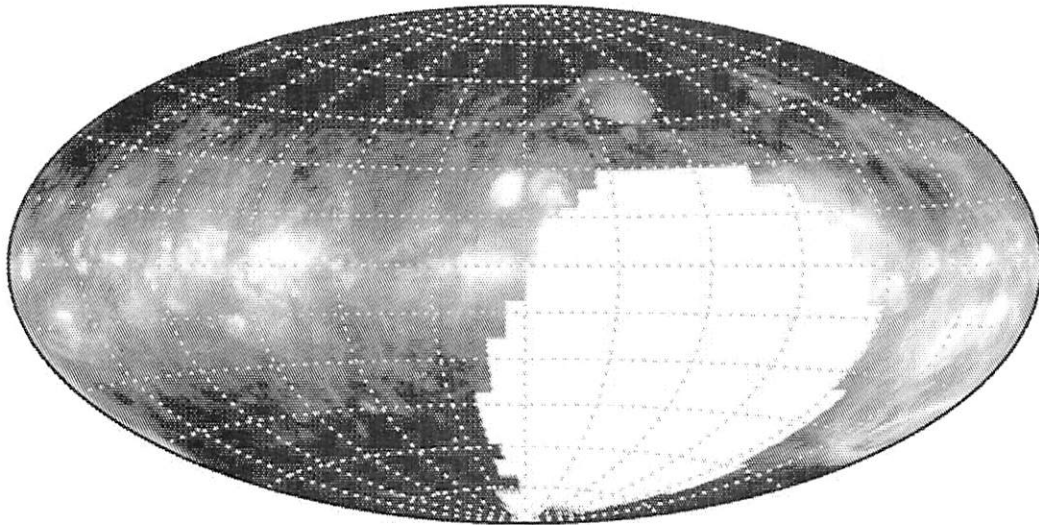
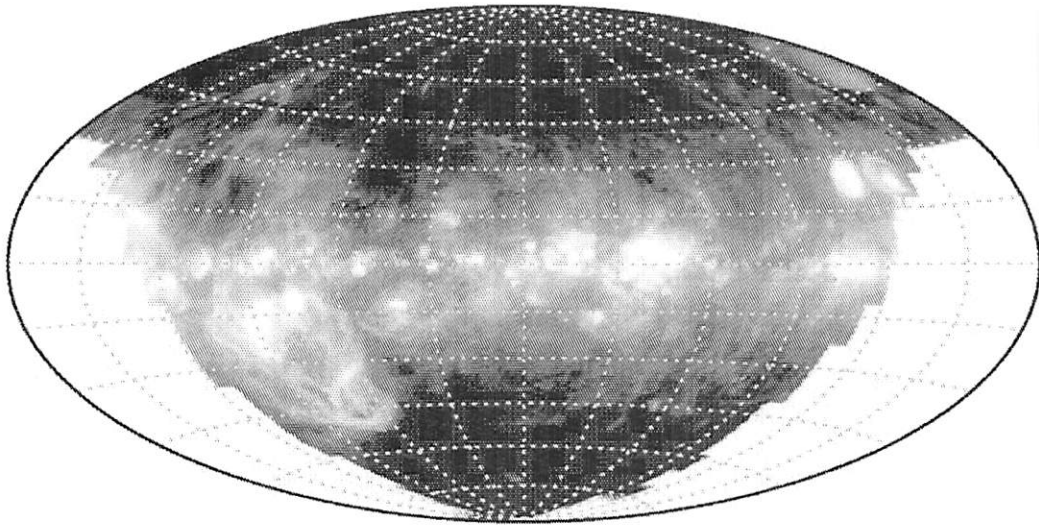
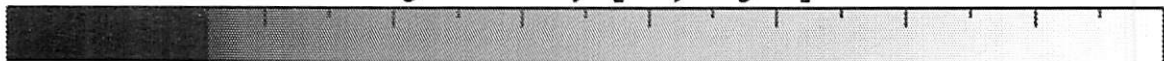


FIG. 1. Composite all-sky velocity-integrated $H\alpha$ map. Data from VTSS, SHASSA, and the WHAM northern sky survey (WHAM-NSS) have been combined to produce these very deep ($EM \geq 1 \text{ cm}^{-6} \text{ pc}$) emission maps. The two Aitoff-Hammer projections are centered at (top) $\ell = 0^\circ$ and (bottom) $\ell = 180^\circ$. Areas covered by the imaging surveys have arc-minute resolution while those only surveyed by WHAM have one-degree resolution. Emission is predominantly from the Galaxy, although the imaging surveys can contain other bright, extended sources from the local universe ($|v_{\text{LSR}}| \lesssim 500 \text{ km s}^{-1}$; LMC, SMC, M31, etc.). Adapted from Finkbeiner, 2003.

along
(DM
d the
rived
($H\alpha$)
e-free
ion of
indi-
n av-
ing a



Log Intensity [Rayleighs]



NGC 157

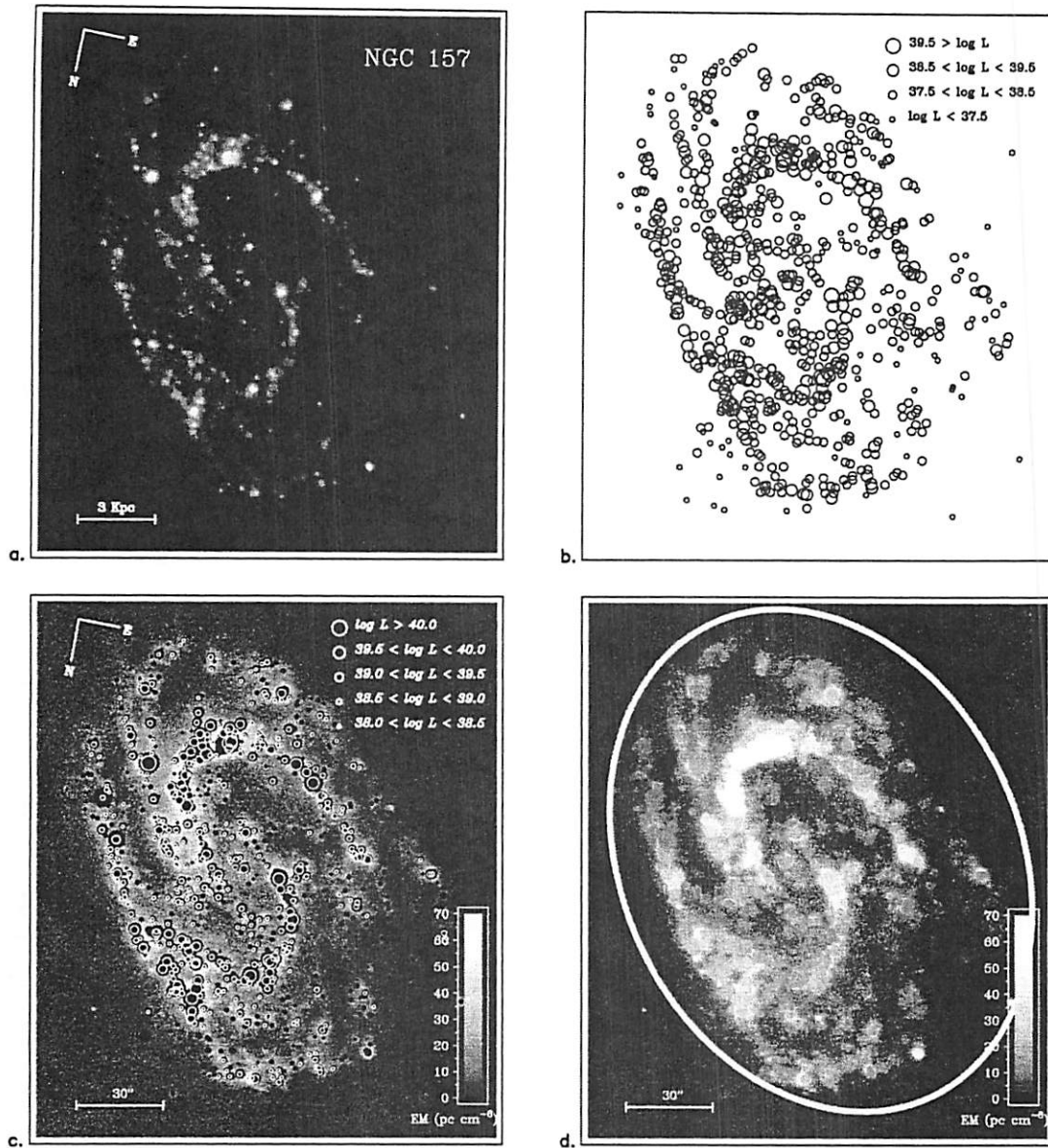


FIG. 9. Steps in the quantification of the total $H\alpha$ luminosity from the DIG for the representative disk galaxy NGC 157. (a) Continuum subtracted $H\alpha$ image. (b) Schematic form of H II region catalog, giving position and key to the $H\alpha$ luminosity of each region. (c) Diffuse $H\alpha$ map after subtracting off the catalogued H II regions. The brightest H II regions are indicated by circles. (d) Measurement of upper limit for DIG. H II regions are blanked off, then each is assigned a local value of DIG surface brightness. Ellipse shows limit of integrated DIG flux measured. From Zurita *et al.*, 2000.

then adding a contribution from the areas of the H II regions, assuming this is proportional to their projected areas times their local DIG surface brightness; or (c), as in (a) but making the contribution proportional to the area of the H II regions times the mean DIG surface brightness outside the regions across the disk of the galaxy. Modes (a), (b), and (c) give, respectively, lower limits, upper limits, and approximate estimates for the total DIG emission from the observed galaxies. In Fig. 11 we show the results of this method of estimating the DIG, for six galaxies, shown as the ratio of the DIG $H\alpha$ luminosity to the total luminosity for the galaxy plotted in terms of galactocentric radius.

We can see that the DIG emits around half of the total $H\alpha$ output, that there are systematic modulations of this tendency with radius, and that there is a slight tendency for the fraction to increase with radius. We also note that the projected area of the disk occupied by the DIG is of order $80(\pm 10)\%$ for all objects shown in Fig. 11. In a separate study of over 100 galaxies, Oey *et al.* (2007) found that the amount of DIG $H\alpha$ to total $H\alpha$ from a galaxy ranged from 20% to nearly 100% with a mean near 60%. Voges (2006) presented results suggesting an inverse correlation between the DIG $H\alpha$ fraction and the star formation rate per unit area.

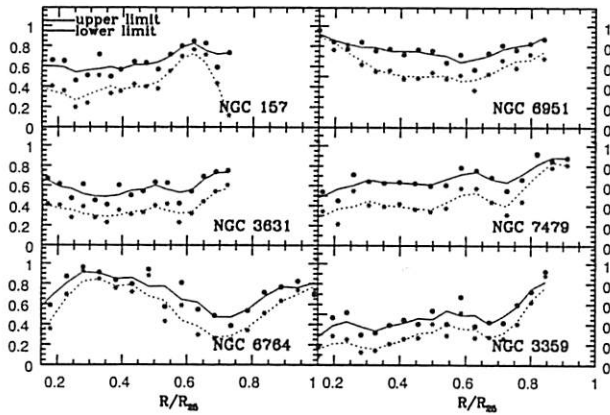


FIG. 11. Radial variation of the ratio of integrated DIG luminosity in $H\alpha$ to the total luminosity for six spiral galaxies (within $0.15R/R_{25}$ crowding precludes accurate estimates). A canonical value for the integrated ratio of $\geq 50\%$ is found, with a total fractional area subtended by the DIG of $\sim 80\%$. From Zurita *et al.*, 2000.

cause of the availability of a VLA H I map of reasonable resolution, as explained shortly. In Fig. 12, we show a comparison between the observed surface brightness distribution in the DIG and one of the simplest models used. In this model, 30% of emitted Lyman continuum photons escape from each H II region, and propagate through the DIG isotropically.

The predicted $H\alpha$ surface brightness is derived by summing the contributions to the ionizing radiation field from each of the H II regions. We can see that the result is remarkably similar globally to the observed distribution, and is itself a fair verification of the initial hypothesis. However, a more quantitative look at the comparison shows that the ratio between the predicted and

observed DIG surface brightness is not uniform on large scales, as would be expected since the initial model assumes a uniform slab structure for the H I involved in converting the Lyman continuum photons to $H\alpha$. The missing structural parameter can be supplied using the observed H I column density, as shown in Fig. 13, where in zones of low H I column density the ratio of observed to predicted DIG surface brightness is reduced. Maps of these two quantities give excellent coincidence of features, and go a step further in showing that the principal DIG ionization sources must be the O stars in luminous H II regions. Modeling the effect of clustered supernovae on the distribution of the H I, Clarke and Oey (2002) also found that the resulting clumpiness of the medium had a significant effect on the escape fraction of the ionizing radiation. Zurita *et al.* (2002) carried out a number of different modeling tests of the basic hypothesis, varying the law relating the escape fraction of ionizing photons with the luminosity of an H II region, and varying the mean absorption coefficient of the inhomogeneous neutral fraction of the DIG. However, they concluded that it was not possible without H I data of improved angular resolution to go further in testing different photon escape laws, or to estimate what fraction of the DIG ionization could be due to mechanisms other than that tested.

C. Line ratio studies

There have been relatively few quantitative spectroscopic studies of the DIG in face-on galaxies. A pioneering study of [N II] and $H\alpha$ across the face of NGC 1068 was carried out by Bland-Hawthorn *et al.* (1991), who found very high [N II]/ $H\alpha$ ratios and discussed possible causes for this high excitation. Hoopes and Walterbos

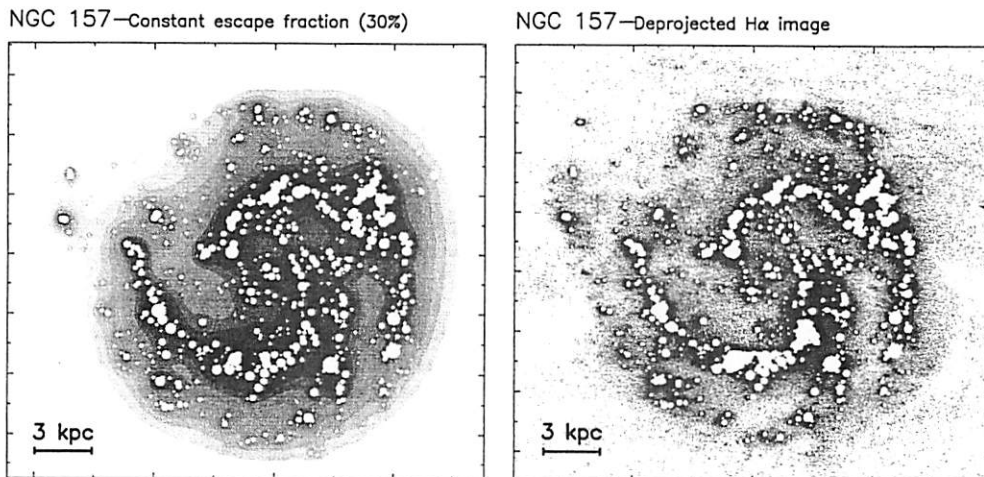
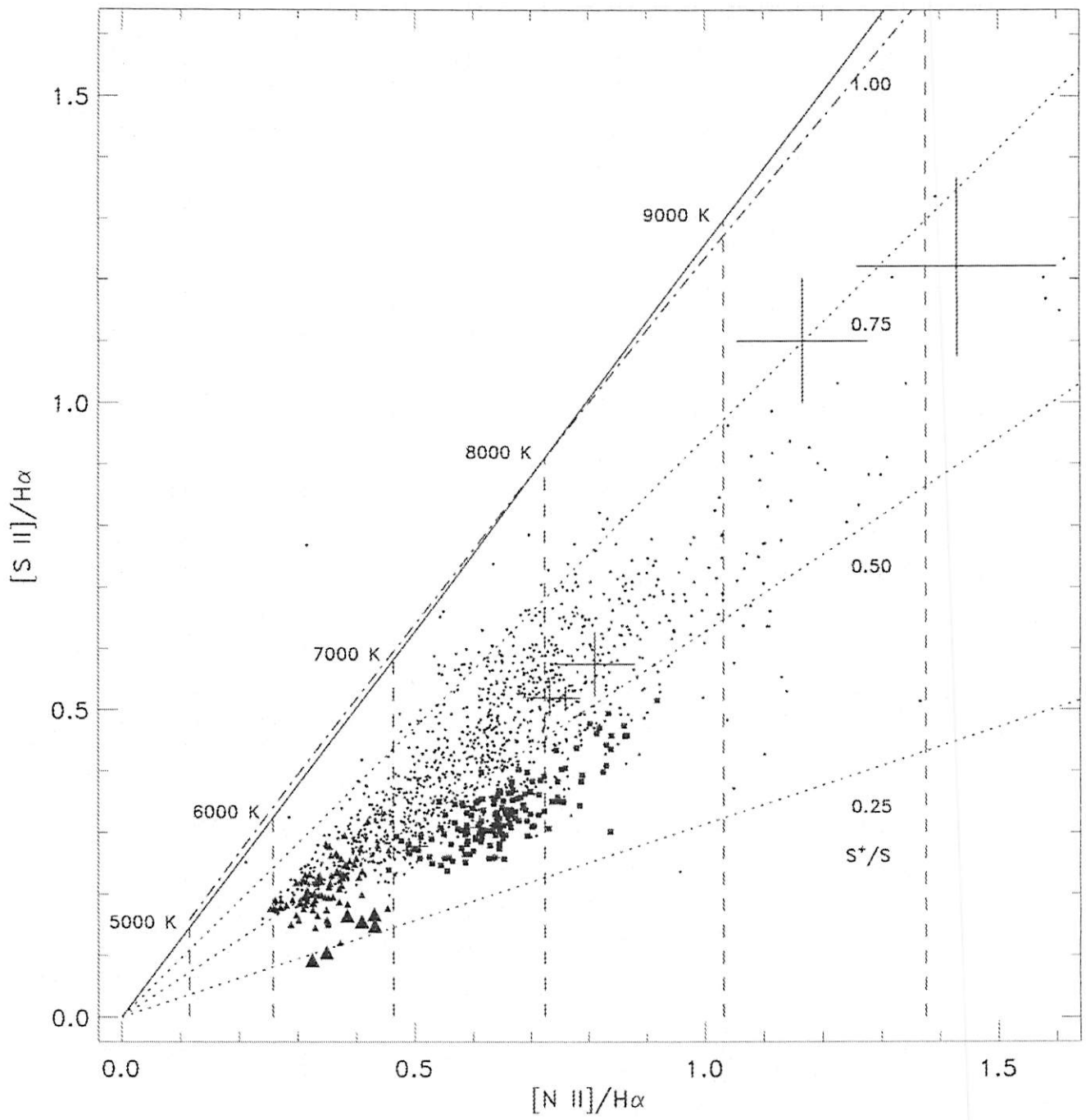


FIG. 12. Comparison of a DIG model with observations. (Left) Modeled surface brightness in $H\alpha$ of the DIG in the disk of NGC 157 assuming 30% of Lyc photons escape from each H II region, and a simple propagation law through a (macroscopically) uniform slab model for the disk. The result is a projection in the plane of the predicted 3D $H\alpha$ column density. (Right) Deprojected image of the galaxy with H II regions masked, and a cutoff of $73 \times \cos i \text{ pc cm}^{-6}$ applied to limit the H II region contamination of the DIG. This shows the basic similarity between these models and the observed DIG, though further refinements are important (see Fig. 13). From Zurita *et al.*, 2002.



The warm ionized medium in spiral galaxies

L. M. Haffner

Department of Astronomy, University of Wisconsin-Madison, Madison, Wisconsin USA, 53706

R.-J. Dettmar

Astronomisches Institut, Ruhr-University Bochum, Germany

J. E. Beckman

*Instituto de Astrofísica de Canarias, Tenerife, Spain
and Consejo Superior de Investigaciones Científicas, Madrid, Spain*

K. Wood

University of St. Andrews, St. Andrews, Scotland

J. D. Slavin

Harvard-Smithsonian Center for Astrophysics, Cambridge, Massachusetts 02138, USA,

C. Giammanco

Instituto de Astrofísica de Canarias, Tenerife, Spain

G. J. Madsen

School of Physics, The University of Sydney, Sydney, NSW 2006, Australia

A. Zurita

Departamento de Física Teórica y del Cosmos, Universidad de Granada, Granada, Spain

R. J. Reynolds

Department of Astronomy, University of Wisconsin-Madison, Madison, Wisconsin 53706, USA

(Published 2 July 2009)

This article reviews observations and models of the diffuse ionized gas that permeates the disk and halo of our Galaxy and others. It was inspired by a series of invited talks presented during an afternoon scientific session of the 65th birthday celebration for Professor Carl Heiles held at Arecibo Observatory in August 2004. This review is in recognition of Carl's long-standing interest in and advocacy for studies of the *ionized* as well as the neutral components of the interstellar medium.

DOI: 10.1103/RevModPhys.81.969

PACS number(s): 98.35.-a, 98.38.-j, 98.58.-w, 95.30.Dr

CONTENTS

I. Introduction	970	Star Formation Rates in Edge-On Galaxies	977
II. View from the Inside: Diving into the Physics of the Warm Ionized Medium in our Galaxy	971	A. Diffuse ionized gas in the halo and star formation in the disk	977
A. Basic characteristics of the WIM and diagnostic tools	971	B. The disk-halo connection and hot gas	977
B. Ionization state	972	IV. Views from the Outside: The Source of the Diffuse Ionized Gas in Face-On Galaxies	979
C. Temperature	973	A. Radiation from O stars and the surface brightness of the DIG	979
1. [N II], [S II], and [O II] with respect to H α	973	B. An escape model for Lyman continuum propagation	981
2. [N II] λ 5755/[N II] λ 6583	975	C. Line ratio studies	982
3. Linewidths	975	V. Modeling the WIM/DIG: Effects of Radiation Transfer Through a Clumpy Interstellar Medium	984
D. Warm ionized and neutral gas	976	A. What exactly is an H II region?	984
E. The role of superbubbles	976	B. Modeling the ionization structure of the DIG	985
III. Views from the Outside: Diffuse Ionized Gas and		1. Escape of ionizing radiation through superbubbles	985

2. Two- and three-dimensional ionization structure of the DIG	985
C. Modeling the emission line spectrum of diffuse ionized gas	986
1. One-dimensional models	987
2. Two- and three-dimensional models	987
3. Interfaces and three-dimensional H II regions	987
4. Leaky H II regions and the He ⁺ /H ⁺ problem	988
VI. Ionizing Radiation from Hot-Gas–Cool-Gas Interfaces	988
A. Types of interfaces	988
B. A test case	989
VII. Some Questions for Future Study	990
A. What is the source of the elevated temperatures?	990
B. What is the spatial distribution of the gas?	990
C. How much ionizing radiation escapes the galaxy?	990
D. Do hot, pre-white dwarf stars play a role?	991
E. Are missing atomic data important?	991
F. What insights will new global models provide?	991
List of Acronyms and Terms	991
Acknowledgments	992
References	993

I. INTRODUCTION

Composed primarily of hydrogen (91% by number) and helium (9%), with trace amounts (0.1%) of heavier elements, the interstellar medium plays a vital role in the cycle of stellar birth and death and galactic evolution. Not only do the properties of the interstellar medium govern the formation of new stars, but through their radiation and the matter and kinetic energy from their outflows and supernovae, these stars in turn determine the properties of the interstellar medium from which the next generation of stars will be born. One of these feedback processes, the subject of this review, is the large-scale ionization of the medium by the youngest and most luminous stars, the O stars. Even though they are located near the galactic midplane in rare, isolated regions of star formation and often surrounded by opaque clouds of neutral hydrogen, the Lyman continuum radiation from these hot stars is somehow able to propagate large distances through the disk and into the galaxy's halo to produce extensive ionization of the interstellar hydrogen. The study of this widespread plasma has impacted our understanding of the dynamic interstellar processes occurring in galaxies.

This area of study began more than four decades ago, when Hoyle and Ellis (1963) proposed the existence of an extensive layer of warm (10^4 K), low-density (10^{-3} cm⁻³) ionized hydrogen surrounding the plane of our Galaxy and having a power requirement comparable to the ionizing luminosity of the Galaxy's O and B stars. Their conclusion was based upon their discovery of a free-free absorption signature in the observations of the Galactic synchrotron background at frequencies between 1.5 and 10 MHz carried out by radio astronomy pioneers Grote Reber and G. R. A. Ellis at Hobart, Tas-

mania (Reber and Ellis, 1956; Ellis *et al.*, 1962). The idea that a significant fraction of the Galaxy's ionizing photons, produced primarily by rare, massive stars residing near the Galactic midplane, traveled hundreds of parsecs throughout the disk to produce widespread ionization conflicted with the traditional picture in which the neutral atomic hydrogen (the primary component of the medium by mass and opaque to hydrogen ionizing radiation) filled much of the interstellar volume. However, less than a decade later, the dispersion of radio signals from newly discovered pulsars (Hewish *et al.*, 1968; Guélin, 1974) plus the detection of faint optical emission lines from the diffuse interstellar medium (Reynolds, 1971; Reynolds *et al.*, 1973) firmly established warm ionized hydrogen as a major, widespread component of our Galaxy's interstellar medium. Two decades later, deep H α imaging with CCD detectors revealed that similar warm plasmas also permeate the disks and halos of other galaxies (Dettmar, 1990; Rand *et al.*, 1990).

The large mass, thickness, and power associated with this ionized layer have modified our understanding of the composition and structure of the interstellar medium and the distribution of Lyman continuum radiation within galaxies. Its weight is a major source of interstellar pressure at the midplane (Boulares and Cox, 1990), and it could be the dominant state of the interstellar medium 1000 pc above the midplane (Reynolds, 1991a). An accurate understanding of interstellar matter and processes thus requires as thorough a knowledge of this diffuse ionized gas as the other principal components of the medium. For a general survey of the interstellar medium, we refer the reader to *The Interstellar Environment of Our Galaxy* by Ferrière (2001) and *The Three Phase Interstellar Medium Revisited* by Cox (2005). Brief review articles on a variety of current interstellar medium topics can be found in *How Does the Galaxy Work?*, a conference proceedings edited by Alfaro *et al.* (2004).

Although the nature of this low-density plasma is not yet fully understood, significant progress has been made in characterizing its properties and the source of its ionization. In Sec. II, we present a brief account of observations of the warm ionized medium (WIM) in our Galaxy, the Milky Way, including results on the physical conditions in the WIM. In Secs. III and IV, we review progress on understanding this gas and its close connection to star formation activity and O stars through studies of other galaxies. O star photoionization models in a clumpy interstellar medium are discussed in Sec. V, with a discussion of supplemental radiation from hot-cool gas interfaces in Sec. VI. A list of some unanswered questions and future challenges is presented in Sec. VII. Throughout we keep the convention that WIM refers to the warm ionized medium in our Galaxy and DIG refers to this diffuse ionized gas in other galaxies. Also, we use H⁺ to refer to the ionized hydrogen in the low-density, widespread WIM/DIG and H II to denote the gas in the localized, higher density, "classical H II regions" immediately surrounding hot stars. For reference, a list of ac-

ronyms and terms with explanations is provided at the end of this paper.

II. VIEW FROM THE INSIDE: DIVING INTO THE PHYSICS OF THE WARM IONIZED MEDIUM IN OUR GALAXY

A. Basic characteristics of the WIM and diagnostic tools

Our location within the disk of the Galaxy provides an opportunity to explore close up and in detail the distribution and physical properties of this ionized medium, including its ionization state and temperature. The basic features of the WIM are not very different from those first proposed by Hoyle and Ellis (1963). Temperatures range from about 6000 to 10 000 K, and in the solar neighborhood, its average hydrogen ionization rate is approximately $4 \times 10^6 \text{ s}^{-1}$ within a 1 cm^2 column extending perpendicular through the Galactic disk, about $\frac{1}{8}$ that available from stellar ionizing photons (see, e.g., Reynolds, 1984; Madsen *et al.*, 2006). The amount of ionization increases toward the Galactic center (see, e.g., Madsen and Reynolds, 2005). In other galaxies, the average ionization rate is observed to be about one-half that available from the stars (see Sec. IV).

Two fundamental parameters of ionized gas along any line of sight s are the dispersion measure ($\text{DM} \equiv \int n_e ds$), derived from pulsar observations, and the emission measure ($\text{EM} \equiv \int n_e n_{\text{H}^+} ds \approx \int n_e^2 ds$), derived from the intensity of the hydrogen Balmer-alpha ($\text{H}\alpha$) recombination line or from the amount of free-free (bremsstrahlung) emission or absorption. Comparison of these measurements along common lines of sight indicates that the H^+ is clumped into regions having an average electron density $n_e = 0.03 - 0.08 \text{ cm}^{-3}$ and filling a fraction $f \approx 0.4 - 0.2$ of the volume within a 2000–3000 pc thick layer about the Galactic midplane (Reynolds, 1991b; Hill *et al.*, 2008). Data also suggest that the filling fraction increases from $f \sim 0.1$ at the midplane to $f > 0.3 - 0.4$ at $|z| = 1000 \text{ pc}$ (Kulkarni and Heiles, 1987; Reynolds, 1991b; Berkhuijsen *et al.*, 2006; Gaensler *et al.*, 2008). The large, 1000–1800 pc scale height, significantly larger than that of the neutral hydrogen layer, has been deduced from both pulsar observations (Reynolds, 1989; Gaensler *et al.*, 2008) and the rate of decrease in the $\text{H}\alpha$ intensity with increasing Galactic latitude for the gas associated with the Perseus spiral arm (e.g., Haffner *et al.*, 1999). The WIM accounts for 90% or more of the ionized hydrogen within the interstellar medium, and along lines of sight at high Galactic latitude (i.e., away from the Galactic midplane), the column density of the H^+ is approximately one-third that of the neutral hydrogen (Reynolds, 1991a).

Although originally detected by radio observations, subsequent developments in high-throughput Fabry-Perot spectroscopy and CCD imaging techniques have demonstrated that the primary source of information on the distribution, kinematics, and other physical properties of the WIM is through the detection and study of

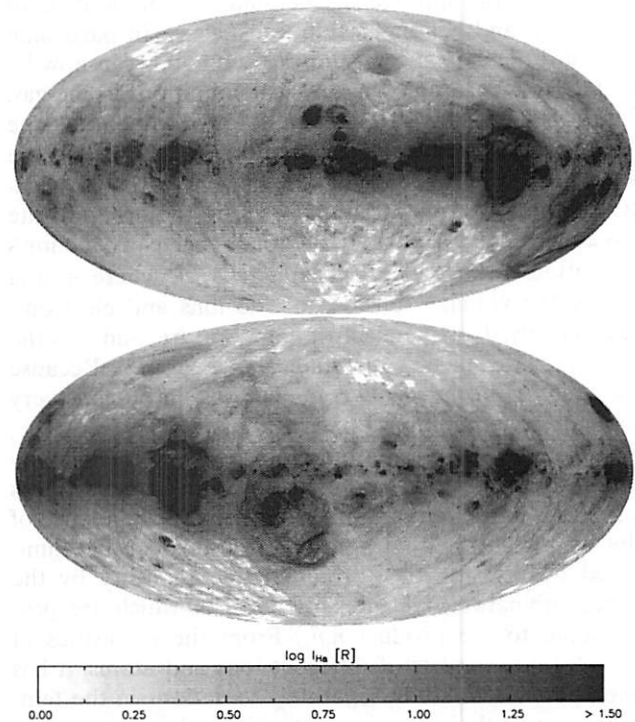


FIG. 1. Composite all-sky velocity-integrated $\text{H}\alpha$ map. Data from VTSS, SHASSA, and the WHAM northern sky survey (WHAM-NSS) have been combined to produce these very deep ($\text{EM} \geq 1 \text{ cm}^{-6} \text{ pc}$) emission maps. The two Aitoff-Hammer projections are centered at (top) $\ell = 0^\circ$ and (bottom) $\ell = 180^\circ$. Areas covered by the imaging surveys have arcminute resolution while those only surveyed by WHAM have one-degree resolution. Emission is predominantly from the Galaxy, although the imaging surveys can contain other bright, extended sources from the local universe ($|v_{\text{LSR}}| \lesssim 500 \text{ km s}^{-1}$; LMC, SMC, M31, etc.). Adapted from Finkbeiner, 2003.

faint interstellar emission lines at optical wavelengths. For example, the distribution of the H^+ is revealed by its interstellar $\text{H}\alpha$ ($\lambda 6563$) recombination line emission, which covers the sky. Several deep $\text{H}\alpha$ surveys have given us our first detailed view of the distribution and kinematics of this gas. Through CCD imaging, Dennison *et al.* (1998) provided partial coverage of the total $\text{H}\alpha$ intensity in the northern sky, while Gaustad *et al.* (2001) covered the southern sky at arcminute resolution and sensitivities around 1 R ($10^6/4\pi \text{ photons cm}^{-2} \text{ s}^{-1} \text{ sr}^{-1}$; $\text{EM} = 2.25 \text{ cm}^{-6} \text{ pc}$ at 8000 K). The Wisconsin H-Alpha Mapper (WHAM) carried out a velocity resolved survey of the northern sky (dec. $> 30^\circ$) at 12 km s^{-1} spectral resolution, 1° spatial resolution, and $\sim 0.1 \text{ R}$ sensitivity (Tuftte, 1997; Haffner *et al.*, 2003). The WHAM maps show WIM emission in virtually every beam, with faint loops, filaments, and blobs of emission superposed on a more diffuse background. Finkbeiner (2003) combined these three surveys to form a composite all-sky view of the velocity-integrated $\text{H}\alpha$ (Fig. 1).

With these new maps and methods for detecting faint emission lines, we are now able to investigate the physical conditions of the WIM, its relationship to other com-

ponents of the interstellar medium, and to sources of ionization and heating within the Galaxy. In particular, standard nebular line diagnostic techniques can now be employed to examine the physical conditions in the gas. In the low-density ($\sim 10^{-1} \text{ cm}^{-3}$) environment of the WIM, the collisional excitation of an ion to a metastable state 2–3 eV above ground by thermal ($\sim 10^4 \text{ K}$) electrons is followed by the decay back to the ground state via a “forbidden” optical transition. Specifically, the ion’s excitation rate $r_i \propto n_i n_e T_e^{-0.5} \exp(-E/kT_e)$, where n_i and n_e are the volume densities of the ions and electrons, respectively, T_e is the electron temperature, and E is the energy of the metastable state above ground. Because thermal equilibrium between electrons and ions is very rapid, the temperature of the ions $T_i = T_e$ (see, e.g., Spitzer, 1978). Thus a variation in the photon emissivity of a forbidden line from one direction to the next traces variations in the temperature, density, and abundance of the ion. The effects of density variations can be eliminated by dividing the forbidden line intensity by the H-recombination line intensity, both of which are proportional to the product $n_i n_e$. From the intensities of lines from a number of different ions and atoms, it has been possible to study separately variations in the temperature and the ionization state within the emitting gas. For many years, these diagnostic techniques have been applied to a variety of astrophysical plasmas [see, e.g., Davidson and Netzer (1979), Osterbrock (1989), Dopita and Sutherland (2003), Ferland (2003), and Osterbrock and Ferland (2006) for in-depth discussions], but only more recently has it been possible to use them to study the much fainter WIM emission lines.

For example, in the WIM, the forbidden lines [S II] $\lambda 6716$ and [N II] $\lambda 6584$ are found to have intensities with respect to $H\alpha$ that range from a few tenths to unity or higher, significantly larger than what is observed for the bright, classical emission nebulae (i.e., H II regions) immediately surrounding O stars. This implies that the physical conditions in the WIM differ significantly from conditions in classical H II regions. In addition, because their intensities are comparable to $H\alpha$, it has been possible to map these lines over large parts of the sky (see, e.g., Madsen *et al.*, 2006). Other lines, such as [N II] $\lambda 5755$, He I $\lambda 5876$, [O III] $\lambda 5007$, and [O I] $\lambda 6300$, are much fainter and have been studied only in a few select directions. These observations have helped to characterize the ionization and temperature of the WIM as well as other extended ionized regions of the Galaxy. Results reveal that not only are the temperature and ionization conditions of the WIM significantly different from the conditions in classical O star H II regions, but that the conditions within the WIM itself vary considerably from one direction to the next and even along a single line of sight (Madsen *et al.*, 2006).

B. Ionization state

The strength of the ionizing radiation field responsible for the WIM can be probed by measuring the $H\alpha$ sur-

face brightness of neutral hydrogen (H I) clouds and by measuring the hydrogen ionization fraction H^+/H within the WIM. Field (1975) pointed out that an H I cloud immersed in an ionizing radiation field will have a skin of H^+ with an emission measure that is directly proportional to the incident photon flux. Using this fact, Reynolds *et al.* (1995) found that an interstellar Lyman continuum flux $4\pi J \approx 2 \times 10^6 \text{ photons cm}^{-2} \text{ s}^{-1}$ could account for most of the WIM’s ionization. This flux implies an ionizing photon density to electron density ratio (the ionization parameter) of 10^{-4} – 10^{-3} , which is one to two orders of magnitude smaller than the ionization parameter in classical O star H II regions. However, values in this range still imply that the hydrogen is nearly fully ionized within the WIM. This is confirmed by more direct measurements of the hydrogen ionization fraction from the detection of neutral oxygen emission.

In theory, directly measuring the degree of H ionization within warm, ionized gas is simply a matter of observing the [O I] $\lambda 6300$ emission line, which is produced by collisions of neutral oxygen with thermal electrons within the WIM. The first ionization potential of O is quite close to that of H (13.595 and 13.614 eV, respectively) and the large $H^+ + O^0 \leftrightarrow H^0 + O^+$ charge-exchange cross section keeps O^+/O nearly equal to H^+/H . Electron energies in $T_e \sim 10^4 \text{ K}$ gas are sufficient to excite the $\sim 2 \text{ eV}$ ($^3P-^1D$) transition that results in the [O I] $\lambda 6300$ emission. Therefore, the intensity of this line relative to $H\alpha$ is directly related to the amount of O^0 , and thus H^0 , relative to H^+ in warm ionized gas (Reynolds *et al.*, 1998). In practice, nature conspires to make this observation very difficult, because [O I] is also one of the brightest terrestrial emission lines in the night sky. Nevertheless, high-sensitivity, high-resolution spectroscopic measurements with WHAM have managed to resolve the Galactic emission from atmospheric emission to provide reliable measurements in a few select directions. These observations indicate that $H^+/H > 90\%$ for $T > 8000 \text{ K}$ (Reynolds *et al.*, 1998; Hausen *et al.*, 2002).

The time scale for recombination at a typical WIM density of 0.1 cm^{-3} is $\approx 1 \text{ Myr}$. This is shorter than the lifetimes of O stars, the presumed ionizing sources, which implies that the photoionization rate of the neutral hydrogen atoms within the WIM is roughly balanced by the rate of hydrogen recombination. In this case, the limit on H^+/H implies an ionizing flux $> 10^5 \text{ photons cm}^{-2} \text{ s}^{-1}$, consistent with the ionizing photon flux derived from the $H\alpha$ surface brightness of H I clouds.

Regarding heavier ions, observations reveal that in the WIM ions are generally in lower states of ionization than in classical O star H II regions (see, e.g., Madsen *et al.*, 2006). The reason is not yet fully understood, since Lyman continuum photons emitted by massive O stars are almost certainly the primary source of ionization for the WIM (see Secs. III and IV). The lower ionization state could be due to a softening of portions of the spectrum as the radiation travels from the O stars to the WIM. Photoionization models (Hoopes and Walterbos,

2003; Wood and Mathis, 2004) showed that the spectral processing of the radiation can be complex, with the radiation between the H I and He I ionization edges hardening with distance from the source, while the spectrum at higher energies softens. Moreover, hot evolved low mass stars (white dwarfs) and interface radiation associated with the hot (10^5 – 10^6 K) gas add harder photons to the mix (Sec. VI). Independent of the spectrum, the low ionization state of the WIM also could be the result of its low ionization parameter (Mathis, 1986).

Constraints on the fluxes of higher energy (i.e., helium-ionizing) photons are from observations of the He I recombination line at $\lambda 5876$ and the [O III] $\lambda 5007$ collisionally excited line. Both of these transitions are prominent in O star H II regions, where $I_\nu(>24 \text{ eV})$ is high enough (and is known to be high enough) to maintain He⁺ (24.6 eV) and O²⁺ (35.1 eV) at appreciable levels. Even qualitatively, from the first attempts to detect these lines in the WIM (Reynolds, 1985a; Reynolds and Tufté, 1995), it was clear that these ions were not as abundant in the WIM. More recent WHAM observations found $(\text{He I}/\text{H}\alpha)_{\text{WIM}} \sim 0.5 \times (\text{He I}/\text{H}\alpha)_{\text{H II}}$, which, when combined with the fact that H⁺/H is near unity (see above), implies that He⁺/He $\leq 60\%$. The [O III]/H α results are more varied, although the ratios are typically less ($\sim 10\%$) than those seen in H II regions (Madsen, 2004; Madsen *et al.*, 2006). The abundance of [O III] in other galaxies and in the interior regions of our Galaxy can be significantly higher than what is observed in the WIM near the Sun (Rand, 1997; Madsen and Reynolds, 2005).

C. Temperature

The temperature of photoionized gas is set by a balance between heating and cooling. Heat is injected by thermalization of the excess kinetic energy of the electron during the photoionization-recombination process [see, e.g., Osterbrock (1989)]. Other potential sources of heat could also be important, particularly at the low densities characteristic of the WIM [see, e.g., Reynolds and Cox (1992)]. Cooling occurs primarily from the collisional excitation and subsequent radiative decay of metastable states (i.e., forbidden lines) of the trace ions [see, e.g., Osterbrock (1989) for a detailed discussion]. The detection of some of these “cooling lines” in combination with the H-recombination emission have been used to explore the temperature of the gas, as discussed below. The observations have established that (i) on average the WIM is about 2000 K warmer than the denser, classical H II regions, and (ii) there are significant variations in temperature within the WIM, most notably an increase in temperature with increasing distance away from the midplane, and, more generally, with decreasing emission measure (or gas density). The reason for this temperature behavior of the WIM is not yet clear; it could indicate that photoionization is not the only important source of heat in the WIM (Reynolds *et al.*, 1999) or that perhaps the spectrum of the ionizing radia-

tion is modified as it propagates far from its source (see Sec. V).

Although they vary in accuracy and difficulty, three tools are available to explore the temperature of the WIM through optical emission lines:

- (i) [N II]/H α and [O II]/H α trace variations in T_e . N⁺, O⁺, and H⁺ are the dominant states of ionization for these elements in the WIM. In addition, their emission lines have different dependences on temperature, so that changes in [N II]/H α and [O II]/H α closely track changes in T_e . Empirically, where $I_{\text{H}\alpha} < 1 \text{ R}$, the brightnesses of the primary optical forbidden lines of [N II], [S II], and [O II] become comparable to H α , making these lines easier to detect and thus attractive diagnostic tools for exploring variations in T_e . Calculating absolute temperatures is more uncertain due to necessary assumptions about the exact ionic fractions and elemental abundances.
- (ii) [N II] $\lambda 5755$ /[N II] $\lambda 6583$ measures T_e directly. The ratio of the “auroral” ($\lambda 5755$) emission line (resulting from excitations to a metastable state 4.0 eV above ground) to that of the much brighter “nebular” ($\lambda 6583$) transition (1.9 eV above ground) allows a derivation of T_e with the fewest assumptions. Since this ratio involves the same ion, it is proportional to $e^{\Delta E/kT_e}$, where ΔE is the difference in the excitation energy of the two states. Near 8000 K, a 2000 K change in temperature produces about a factor of 2 change in the ratio. However, because $I_{5755}/I_{6583} \sim 0.01$, this observation is extremely difficult for the WIM, where $I_{\text{H}\alpha} \sim 1 \text{ R}$.
- (iii) Widths of resolved line profiles are proportional to T_i . Comparing the width of the H α line to the width of an emission line from the heavier N⁺ or S⁺ ion can be used to separate the thermal from the nonthermal motions in the gas. However, very high signal-to-noise ratio line profile measurements are needed because the derived value of the ion temperature T_i is proportional to the difference of the squares of the linewidths.

Results using these techniques in recent observations are summarized below.

1. [N II], [S II], and [O II] with respect to H α

Two robust statements can be made about the line ratio observations:

- (a) [N II]/H α , [S II]/H α , and [O II]/H α increase with decreasing $I_{\text{H}\alpha}$. In the Galaxy, this rise is most dramatic below $I_{\text{H}\alpha} = 1 \text{ R}$. The clearest examples of this are the large increases in the forbidden line intensities relative to H α with increasing distance from the midplane, both in our Galaxy (Haffner *et al.*, 1999) and others (Rand, 1998; Tüllmann *et al.*, 2000).

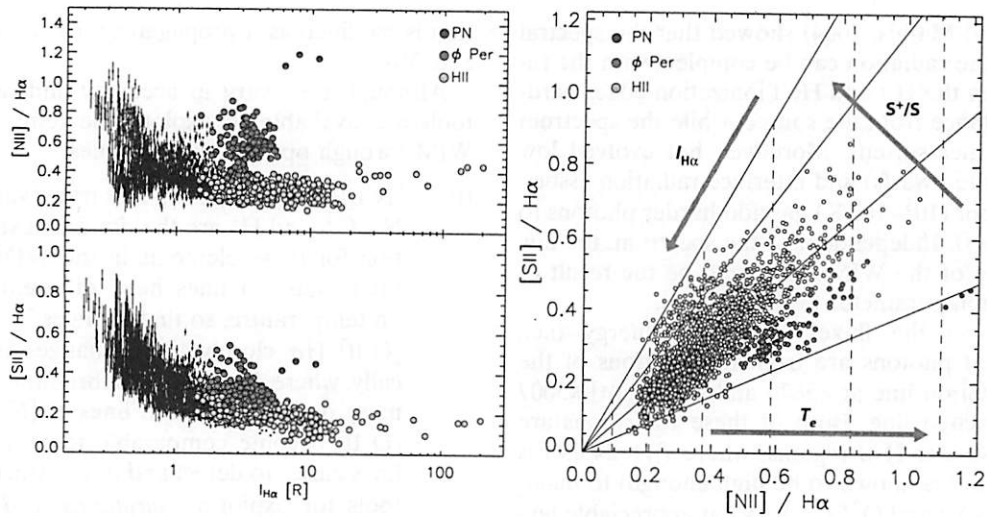


FIG. 2. Diagnostic line ratio diagrams. A large portion of the Galaxy in the direction of the Perseus arm ($\ell=130^\circ$ to 160° and $b=-30^\circ$ to $+30^\circ$, approximately) has been surveyed in $H\alpha$, $[S\ II]$, and $[N\ II]$ with WHAM. These panels show (left) the relationship between the ratios vs the intensity of $H\alpha$ as well as (right) the relationship between the two ratios for the “local” gas component ($|\nu_{LSR}| < 15\text{ km s}^{-1}$). A few specific spatial regions are highlighted with grayscale fill to show the effects of local ionizing sources: the planetary nebula (PN) S216, the H II region surrounding the B0.5+sdO system ϕ Per, and regions near O-star H II regions. Other data points sample the WIM. In the diagram on the right, the vertical dashed lines represent $T_e=5000, 6000, 7000, 8000, 9000,$ and $10\,000\text{ K}$, from left to right. The slanted solid lines represent $S^+/S=0.25, 0.50, 0.75,$ and 1.00 , lowest to highest slope. These WIM data reveal significant variations in T_e and S^+/S from one line of sight to the next. In contrast, classical H II regions all cluster in the lower left corner of this diagram near $[N\ II]/H\alpha \approx 0.25$, $[S\ II]/H\alpha \approx 0.1$. From Madsen, 2004.

- (b) Values for $[S\ II]/H\alpha$ and $[N\ II]/H\alpha$ vary greatly, but are strongly correlated, often with a nearly constant $[S\ II]/[N\ II]$ ratio over large regions. For the Galaxy, the ratio of $[S\ II]/[N\ II]$ does not vary by more than about a factor of 2, except in the vicinity of a discrete ionizing source (e.g., an O star).

As pointed out by Haffner *et al.* (1999), this behavior suggests that changes in the line ratios are due primarily to changes in T_e . Thus statement (b) above follows from the fact that the $[S\ II]$ and $[N\ II]$ lines have nearly identical excitation energies, so that

$$\frac{I_{6716}}{I_{6583}} = 4.69 \frac{(S/H)}{(N/H)} \frac{(S^+/S)}{(N^+/N)} e^{0.04/T_4} T_4^{-0.119}, \quad (1)$$

which is only a very weak function of T_4 ($\equiv T_e/10^4\text{ K}$). From $T_4=0.5$ to 1.0 with all else constant, $[S\ II]/[N\ II]$ decreases only about 11%. This relationship also indicates that the relatively small but real variations of $[S\ II]/[N\ II]$ that are observed in the WIM are tracing variations of S^+/N^+ . Combined with the very different energies required for $S^+ \rightarrow S^{2+}$ (23.3 eV) and $N^+ \rightarrow N^{2+}$ (29.6 eV), we conclude that S^+/S , and especially N^+/N , vary little in the WIM and that the smaller (factor of 2) variations in $[S\ II]/[N\ II]$ are due primarily to variations in S^+/S . This is supported by photoionization models (see, e.g., Sembach *et al.*, 2000), which have shown that $N^+/N \approx 0.8$ over a wide range of input spectra and ionization parameters.

On the other hand, the strong temperature dependence of the forbidden line intensities relative to $H\alpha$ is illustrated by the relationship for $[N\ II]/H\alpha$,

$$\frac{I_{6583}}{I_{H\alpha}} = 1.63 \times 10^5 \left(\frac{H^+}{H}\right)^{-1} \left(\frac{N}{H}\right) \left(\frac{N^+}{N}\right) T_4^{0.426} e^{-2.18/T_4}. \quad (2)$$

Because N^+/N and H^+/H vary little within the WIM, variations in $[N\ II]/H\alpha$ essentially trace variations in T_e . Similar relationships can be written for $[O\ II]$, $[S\ II]$, and for other collisionally excited lines (see Otte *et al.*, 2001).

Using Eqs. (1) and (2), we can construct diagnostic diagrams as presented by Haffner *et al.* (1999) and Madsen *et al.* (2006) to estimate both T_e and S^+/S from observations of $[N\ II]/H\alpha$ and $[S\ II]/H\alpha$, as shown in Fig. 2 [adapted from Madsen (2004)]. With sufficient velocity resolution it has even been possible to study variations in these parameters between different radial velocity components along the same line of sight. These results reveal that within the WIM there are variations in temperatures ranging between about 7000 and 10 000 K and variations in S^+/S between 0.3 and 0.7. For comparison, the bright classical H II regions all cluster near the lower left corner of the plot, $[S\ II]/H\alpha \approx 0.1$ and $[N\ II]/H\alpha \approx 0.25$, where $T_e=6000\text{--}7000\text{ K}$ and $S^+/S \approx 0.25$.

$[O\ II]$ at $\lambda 3727$ has a larger excitation energy than $[N\ II]$, making it even more sensitive to variations in T_e . Although inaccessible with WHAM, several extragalactic studies (Tüllmann and Dettmar, 2000; Otte *et al.*, 2001, 2002) have traced this line, and new instrumentation is starting to allow studies of $[O\ II]$ from the WIM (Mierkiewicz *et al.*, 2006) of the Milky Way. The $[O\ II]$ observations confirm that the line ratio variations are dominated by variations in T_e .

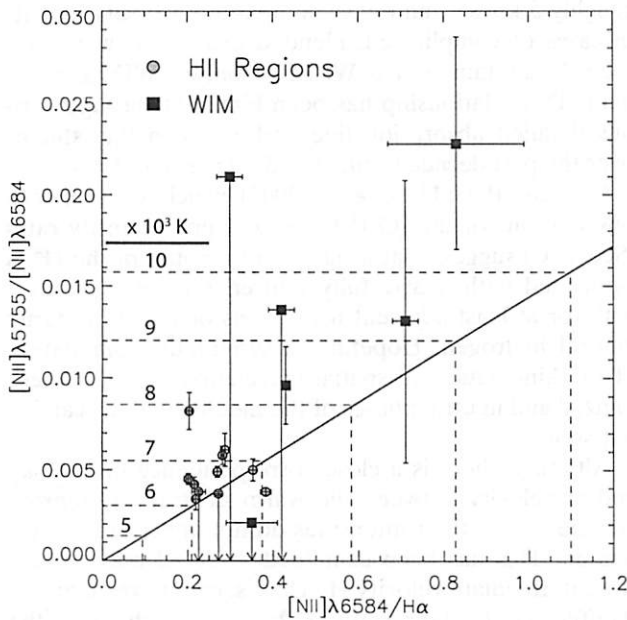


FIG. 3. Elevated temperature in the WIM. Select directions toward (■) brighter diffuse ionized regions show elevated line ratios in both $[\text{N II}]\lambda 5755/[\text{N II}]\lambda 6584$ compared to (○) H II regions. Dashed lines mark select temperatures derived from each line ratio while the diagonal line traces “unity” in this derived temperature space. WIM directions have higher derived temperatures using either line ratio, but are also systematically above the line of unity, suggesting that measurable temperature inhomogeneities exist along these lines of sight. From Madsen, 2004.

2. $[\text{N II}]\lambda 5755/[\text{N II}]\lambda 6583$

One of the most direct ways of measuring T_e in ionized gas is to observe the ratio of two emission lines from the same ion but with very different excitation energies above ground. The I_{4363}/I_{5007} ratio of $[\text{O III}]$ in bright H II regions is perhaps the most famous of these pairs. In the WIM, because the $[\text{O III}]/\text{H}\alpha$ ratios are typically no more than 10% of that in H II regions, the isoelectronically similar $[\text{N II}]$ line ratio I_{5755}/I_{6583} has been used instead.

By detecting this extremely weak line, Reynolds, Sterling, Haffner, *et al.* (2001) and Madsen (2004) confirmed in select directions that T_e in the WIM is indeed higher by about 2000 K than in the bright H II regions. However, the details of the results reveal a more complicated temperature structure—perhaps not surprisingly. Although current measurements of the $\lambda 5755$ line still have large uncertainties, Fig. 3 indicates that T_e as inferred by the ratio of the $[\text{N II}]$ lines is systematically higher than that inferred by $[\text{N II}]/\text{H}\alpha$ in the same directions. This could be explained by temperature variations along the line of sight, since the $\lambda 5755$ line (excitation energy 4 eV) would be produced preferentially in regions with higher T_e compared to the red line (2 eV).

3. Linewidths

If the intrinsic widths of emission lines can be measured accurately in ions having significantly different

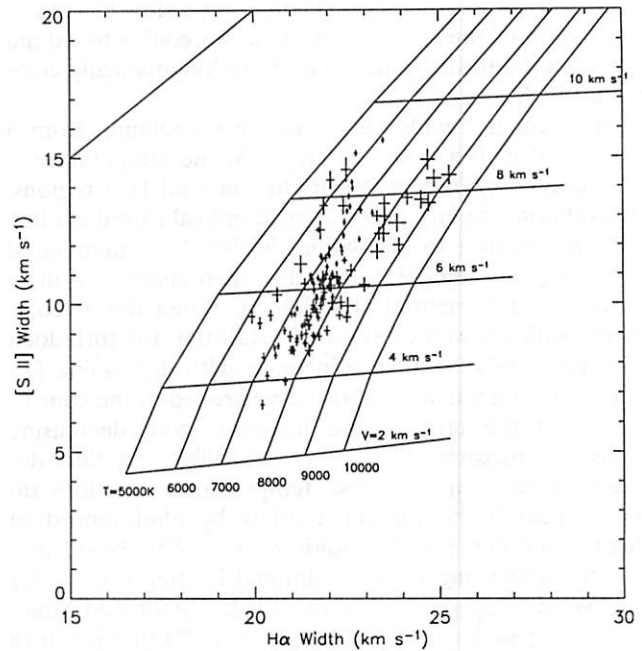


FIG. 4. Temperature T_i and the mode v_{NT} (most probable value) of the nonthermal speed distribution of the diffuse H II region surrounding ζ Oph. The primary axes show the measured widths and errors of $\text{H}\alpha$ and $[\text{S II}]$ from 126 one-degree pointings obtained by WHAM within a 12-degree diameter region around ζ Oph. A grid of temperatures and nonthermal velocities has been superimposed to show the distribution of T_i and v_{NT} within the H II region. The apparent scatter in these values is spatially correlated (see text). The line at the upper left is the line of equal widths.

masses, then one can decompose the thermal motion (i.e., T_i) and nonthermal motion contributing to their widths. H and S are particularly good to use because they differ in mass by a factor of 32, resulting in a measurable difference in their widths. This method has been used with some success in both the WIM (Reynolds, 1985b) and H II regions (Reynolds, 1988).

The potential power of this technique is illustrated in Fig. 4, which shows linewidth data for the large, high Galactic latitude H II region surrounding the O star (O9.5 V) ζ Oph. The $\text{H}\alpha$ from this region spans an order of magnitude in intensity and at the fainter end becomes comparable to WIM emission at low Galactic latitudes (~ 10 R). The ζ Oph H II region is particularly good for linewidth studies because each emission line profile is well described by a single Gaussian component. Baker *et al.* (2004) measured the widths of the $\text{H}\alpha$, $[\text{S II}]$, and $[\text{N II}]$ emission lines from this region and derived accurate values for the temperature T_i and the mode of the nonthermal speeds v_{NT} as shown in Fig. 4. The large ranges in these parameters appear to be real, with a noticeable gradient of increasing T_i (from 6000 to 8000 K) and decreasing v_{NT} (from 8 to 4 km s^{-1}) from the center to edge of the H II region. The former is ascribed to the hardening of the radiation field with increasing distance from the source (Wood *et al.*, 2005; see also Sec. V),

while the latter could be explained by a slow (2 km s^{-1}) expansion of the H II region. A future goal is to extend this method to the fainter and more kinematically complex WIM.

In summary, evidence is now overwhelming from a variety of methods that in the WIM the temperature is elevated compared to the bright, classical H II regions. In addition, the large variations in optical forbidden line strength relative to $H\alpha$ within the WIM are dominated by changes in temperature rather than changes in ionic fractions or elemental abundances. When this is combined with the well-established result that the forbidden line ratios relative to $H\alpha$ increase with decreasing $H\alpha$ intensity [statement (a) above], we are led to the conclusion that the temperature increases with decreasing emission measure (Haffner *et al.*, 1999) and thus decreasing gas density. These temperature variations do not appear to be explained solely by photoionization heating of the gas (Reynolds *et al.*, 1999; Wood and Mathis, 2004), suggesting additional heating sources for the WIM (Reynolds and Cox, 1992; Minter and Spangler, 1997; Weingartner and Draine, 2001) that begin to dominate over photoionization heating at low densities ($\sim 10^{-1} \text{ cm}^{-3}$).

D. Warm ionized and neutral gas

The fact that hydrogen is nearly fully ionized within the $H\alpha$ emitting gas (Sec. II.B) implies that H^+ and H^0 are primarily confined to separate regions. With the advent of velocity-resolved $H\alpha$ surveys (i.e., WHAM), it is now possible to begin to explore the relationship between the diffuse ionized gas and neutral gas in the interstellar medium. Is the WIM the ionized portion of a low-density “intercloud medium” (Miller and Cox, 1993) or is it mostly confined to the surfaces of neutral clouds, the transition region between cooler gas and a much hotter “coronal” temperature medium (McKee and Ostriker, 1977)? Do the ionized and neutral phases cycle from one to the other? Cox and Helenius (2003) and Lockman (2004) suggested that portions of the ionized medium may condense into neutral clouds. However, to date there have been no observational studies of the H^+ - H^0 connection. In a general qualitative sense, a comparison of the optical line profiles with the radio 21 cm (H I) profiles (see, e.g., Hartmann and Burton, 1997) indicates that at high latitudes the ionized gas tends to be correlated in space and velocity with the so-called warm neutral medium (WNM), the widespread, $T \sim 10^3 \text{ K}$ phase of the H I generally associated with broad 21 cm profiles. There is little correspondence between the $H\alpha$ and the narrow-line 21 cm emission components associated with the colder ($T \sim 10^2 \text{ K}$), denser H I clouds. In regions of the sky that contain anomalous velocity structures, specifically, the intermediate and high velocity clouds that are not corotating with the Galactic disk, the correlation is quite strong (Tufté *et al.*, 1998; Haffner *et al.*, 2001). The optical and radio emission components are centered at nearly the same velocities (within

roughly 5 km s^{-1}) and have comparable velocity extents in cases of complicated, blended profiles. Few regions seem to contain only a WNM or only a WIM component. This relationship has been hinted at through various detailed absorption line and emission line studies over the past decade (Spitzer and Fitzpatrick, 1993; Reynolds *et al.*, 1995; Howk *et al.*, 2003), which together with observations of the [O I] $\lambda 6300/H\alpha$ line intensity ratio (Sec. II.C) suggest that a significant amount of the H^+ is associated with nearly fully ionized regions in contact with (or at least adjacent to) regions of warm primarily neutral hydrogen. Hopefully a systematic examination of the kinematic and spatial correlation between these ionized and neutral phases of the medium will be carried out soon.

Although there is a close correspondence on the sky and in velocity between the warm neutral and ionized emission lines, their intensities do not appear to be correlated. This has been examined in detail only toward two intermediate velocity H I clouds, complexes L and K (Haffner *et al.*, 2001; Haffner, 2005). In both cases, the column density of the neutral hydrogen $N_{H\text{I}}$ and that of the $H\alpha$ intensity $I_{H\alpha}$ are uncorrelated. Whether this holds for more local gas in the Galactic disk still needs to be fully explored. A straightforward explanation for this lack of correlation is the fact that the intensity of the $H\alpha$ is determined solely by the flux of ionizing radiation incident on the warm H I cloud (Reynolds *et al.*, 1995), which, of course, is independent of the cloud’s column density because the H I clouds are optically thick to the Lyman continuum photons.

E. The role of superbubbles

One of the basic questions concerning the nature of the WIM is how ionizing photons from O stars can travel hundreds of parsecs through the disk and into the halo. A fractal morphology of the interstellar medium is one possibility (see Sec. V). Another is the existence of enormous, H I-free bubbles surrounding some of the O stars, which allow the Lyman continuum photons to travel through the cavity to ionize its distant walls (see, e.g., Reynolds and Ogden, 1979; Norman and Ikeuchi, 1989; McClure-Griffiths *et al.*, 2006; Pidopryhora *et al.*, 2007). A WHAM study of one of these bubbles, the Perseus superbubble (Reynolds, Sterling, and Haffner, 2001; Madsen *et al.*, 2006), has shown that a luminous O-star cluster near the midplane can indeed produce widespread, nearly WIM-like ionization conditions out to distances of 1000 pc or more from the ionizing stars. However, the [N II]/ $H\alpha$ and [S II]/ $H\alpha$ ratios of the superbubble wall are not quite as large as the ratios observed in the surrounding WIM, suggesting that bubble size, gas density within the shell, supplemental heating, and/or the flux and spectrum of the radiation escaping the O-star cluster may also be important in setting the conditions of the ionized gas.

III. VIEWS FROM THE OUTSIDE: DIFFUSE IONIZED GAS AND STAR FORMATION RATES IN EDGE-ON GALAXIES

In galaxies other than our own, the widespread H^+ is most often referred to as the diffuse ionized gas (DIG). While its physical properties can be measured in much more detail for the interstellar medium of our Galaxy, the detection of the DIG in other galaxies provides the much needed “outside” perspective. Rand (1997, 1998) detected the DIG far into the halo of the edge-on spiral galaxy NGC 891 and found that not only was $[S\ II]/H\alpha$ anomalously high, as observed in the solar neighborhood, but that $[S\ II]/H\alpha$, $[N\ II]/H\alpha$, and even $[O\ III]/H\alpha$ increased significantly with increasing distance from the midplane. This opened up a broader discussion about the ionization and heating processes within the gas and their variation with location within a galaxy.

Furthermore, observations of other galaxies provide important new information about the links between the DIG and global properties of galaxies, such as their star formation activity. In particular, the structure of this gas perpendicular to the galactic plane, that is, in the main direction of the gravitational potential, is an excellent tracer of the dynamics of the interstellar medium driven by energetic galactic processes. The observations corroborate the picture of a dynamic interstellar medium driven by multiple and clustered supernova, producing the so-called disk-halo interaction between the star formation regions near the midplane and energized interstellar matter that extends a kiloparsec or more above the disk. Early discussions of these ideas can be found in *Supernovae, the Interstellar Medium, and the Gaseous Halo: The Swashbuckler’s Approach* by Heiles (1986), *The disk-halo interaction—Superbubbles and the structure of the interstellar medium* by Norman and Ikeuchi (1989), and *Galactic worms* by Koo *et al.* (1992).

A. Diffuse ionized gas in the halo and star formation in the disk

From an observational point of view, the study of the warm H^+ in galactic halos—the extraplanar diffuse ionized gas—is a good start toward understanding the nature of gaseous halos and the disk-halo connection. Of all tracers of halo gas, the warm ionized gas is the easiest to observe with regard to sensitivity and resolution (Dettmar, 1992, 1998; Rand, 1997, 1998), allowing us to study the global influence of the energy released by young and massive stars into the interstellar medium.

A halo component of the DIG for external galaxies was first discovered in NGC 891 (Dettmar, 1990; Rand *et al.*, 1990), followed by studies of a number of other galaxies (see, e.g., Pildis *et al.*, 1994; Rand, 1996; Rossa and Dettmar, 2000). Rossa and Dettmar (2003a, 2003b), used a large sample of edge-on spiral galaxies for a correlation of DIG in the halo with the star formation rate (SFR) in the disk [see also Miller and Veilleux (2003) for comparison]. This survey covered a broad range in SFR

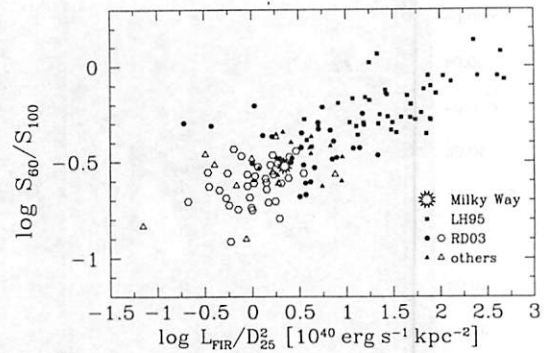


FIG. 5. The dependence of DIG detections in halos of galaxies on the normalized star formation rate (per unit area). The ratio of the FIR fluxes at 60 and 100 μm (S_{60}/S_{100}) is given vs the FIR luminosity normalized to the optical galaxy diameter at 25th mag in units of $10^{40} \text{ erg s}^{-1} \text{ kpc}^{-2}$. Filled symbols indicate detections of H^+ gas in the halo while open symbols represent nondetections. Galaxies from the (■) starburst sample of Lehnert and Heckman (1995) are included with more normal spirals. Integrated values for the Galaxy are from Bloemen *et al.* (1990) and Cox and Mezger (1989) for the FIR. A galactic disk radius of 22.5 kpc is assumed. Adapted from Rossa and Dettmar, 2003a.

extending the observations to less active galaxies. Until then, emphasis had been given mainly to galaxies with high SFR or even starburst galaxies (Lehnert and Heckman, 1995). This relationship between the presence of DIG and far-infrared (FIR) emission (a measure of the SFR) is shown in Fig. 5. If the star formation rate per unit area is low, as determined by the FIR luminosity normalized to the disk surface area, the presence of halo DIG indeed is observed to diminish.

The FIR luminosity per unit area, therefore, seems to be a promising indicator for the presence of halo H^+ and suggests that there is a minimum SFR per area required to drive the disk-halo interaction (Rossa and Dettmar, 2003a). Given the known large uncertainties in the normalization of supernova rates from FIR fluxes, a reasonable estimate for the local break-out condition is on the order of ~ 15 SNe over the lifetime of the O star association. An obvious shortcoming of this analysis is the use of global measurements for the FIR luminosities. Future observations with higher angular resolution, for example, with the Spitzer satellite, could allow a much better comparison of the local SFR with associated halo gas properties.

B. The disk-halo connection and hot gas

The scenario of the disk-halo connection predicts outflows of hot (10^6 K), supernova-created gas away from the disk and into the halo via superbubbles (or “chimneys”). In this way, transparent (i.e., $H\ I$ -free) pathways are then also provided for the transport of ionizing radiation into the halo and beyond. For galaxies with strong starburst activity, this is well supported by observations (see, e.g., Cecil *et al.*, 2002; Strickland *et al.*, 2004a, 2004b; Veilleux *et al.*, 2005) and described well by

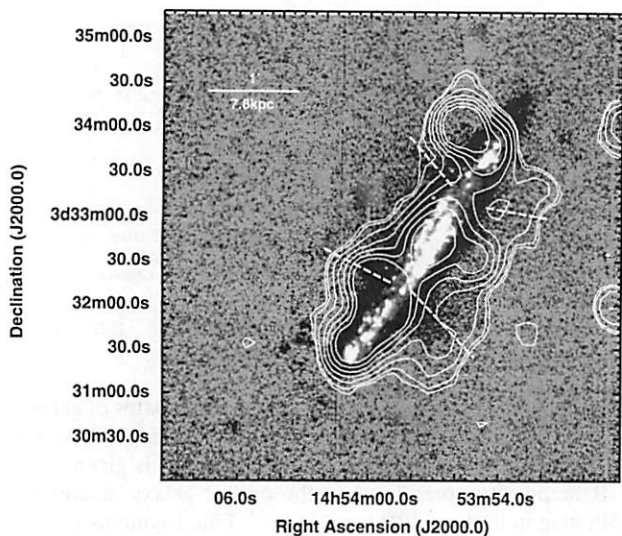


FIG. 6. The x-ray halo NGC 5775 from integrated EPIC XMM-Newton observations exhibits substructure correlating on galactic scales with filaments of diffuse ionized gas and spurs in the radiocontinuum. Adapted from Tüllmann *et al.*, 2006.

theory and numerical modeling (see, e.g., Mac Low and Ferrara, 1999). However, for more normal (i.e., nonstarburst) galaxies, we have little direct evidence for such outflows. High-resolution ground-based (see, e.g., Howk and Savage, 2000) and HST imaging (e.g., Rossa *et al.*, 2004) studies of the DIG distribution in edge-on galaxies do not reveal the number and specific morphology of superbubblelike chimneylike structures predicted by some models (Norman and Ikeuchi, 1989). Such structures have been found, but their number is small. The difficulty in finding them could be an observational problem, e.g., confusion due to superpositions along the line of sight, or it could mean the the current models of the disk-halo connection need further work. Thus, the idea of actual mass exchange between disk and halo is still only a working hypothesis.

On the other hand, there is circumstantial evidence for hot gas outflows in more normal disk galaxies that is indicated by the detection of diffuse interstellar x-ray emission, both in our Galaxy (see, e.g., Smith *et al.*, 2007) and others (see, e.g., Wang *et al.*, 2001). In a sample by Ranalli *et al.* (2003) that included disk galaxies with more normal star formation rates, a correlation was found between the galaxy's global x-ray emission, presumably associated with the very hot (10^6 K) gas located inside supernova remnants and superbubbles, and the amount of star formation activity in the disk. With the current generation of x-ray satellites it is now possible to extend the x-ray studies from the starbursting and luminous galaxies to less active galaxies. One result of a small survey with XMM-Newton is shown in Fig. 6. The EPIC x-ray image of the galaxy NGC 5775 is integrated over all energies and summed over all detectors. It demonstrates the presence of smaller scale x-ray emission features associated with $H\alpha$ filaments far above the disk.

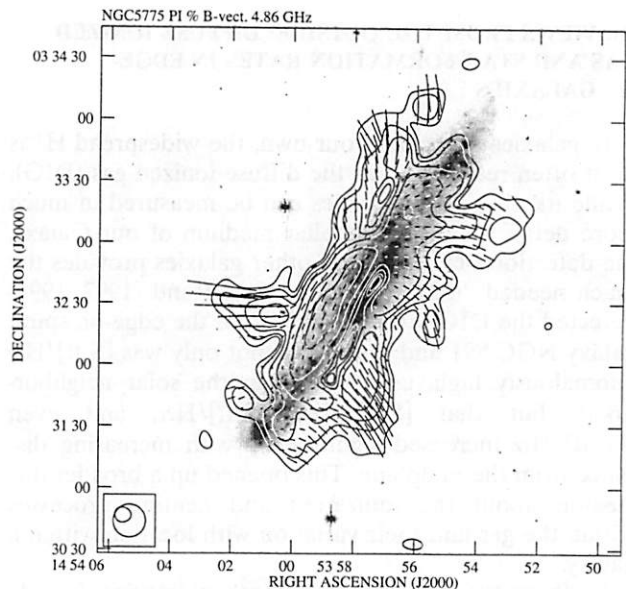


FIG. 7. VLA radiocontinuum map of NGC 5775 at 6 cm. The polarized intensity is given in contours on a gray scale representation of the $H\alpha$ emission. The bars represent the magnetic-field direction and strength. Adapted from Tüllmann *et al.*, 2000, courtesy M. Soida.

The diffuse H^+ in galactic halos is, in most of the observed cases, also associated with synchrotron radiocontinuum halos, suggesting that there is also a relationship between DIG and the presence of cosmic rays and magnetic fields in the halo. For example, NGC 5775 shows a prominent radio continuum halo, and a study of its polarization characteristics with the Very Large Array (VLA) radio synthesis telescope reveals a highly structured large-scale magnetic field with an ordered component to the field lines that opens up into the halo (Fig. 7). This particular structure of the magnetic field could be of interest for the interpretation of global dynamo theory in galaxies and has been discussed by Beck *et al.* (1996). The condition that allows cosmic rays to break out of the disk as a function of star formation rate per unit area has been discussed by Dahlem *et al.* (1995). A detailed study of the kinematics of the DIG in NGC 5775 has been presented by Heald *et al.* (2006). A compilation of observations of edge-on galaxies in $H\alpha$, radio continuum, and x rays has been given by Dettmar (1998) and Rossa and Dettmar (2003a, 2003b).

In summary, studies of edge-on galaxies have shown that warm ionized gas halos are found in galaxies where the SFR per unit area is sufficiently high. Typically these layers of extraplanar DIG can be traced out to distances of $z \approx 1000$ – 2000 pc, sometimes even up to 5000 pc or more from the midplane of the disk. The H^+ halos seem to be associated with halos of cosmic rays and x-ray emitting plasma, which is expected if a superbubble or chimneys provide absorption-free pathways for hydrogen ionizing photons as well as being conduits for the vertical transport of hot gas and cosmic rays away from the disk and into the halo.

IV. VIEWS FROM THE OUTSIDE: THE SOURCE OF THE DIFFUSE IONIZED GAS IN FACE-ON GALAXIES

Observations of edge-on and face-on galaxies clearly provide complementary perspectives of the distribution of the DIG. Specifically, face-on galaxies show the surface brightness of emission lines from the DIG across the face of the galaxy, which makes it possible to explore relationships (if any) between the properties of this plasma and the locations and ionizing fluxes of the hot, massive O stars, which are the most powerful ionizing agents in disk galaxies and are the presumed ionizing source for the DIG. In general, the observations reveal a strong relationship with the $H\alpha$ flux from the DIG comparable to that from the classical O star H II regions in the galaxy.

The presence of diffuse interstellar $H\alpha$ emission in face-on spirals was first noted by Monnet (1971), who derived a temperature of 7000 K, an emission measure of about $35 \text{ cm}^{-6} \text{ pc}$, and a density near 0.5 cm^{-3} for the emitting gas. Modern detector technology (i.e., CCDs) has pushed the detection of diffuse H^+ to fainter regions and has allowed the study of other emission lines, which has provided insight into the relationship between the diffuse ionization and the O stars.

A. Radiation from O stars and the surface brightness of the DIG

Although it was not understood how Lyman continuum photons could have free paths of hundreds of parsecs and more in galaxies with typical interstellar H I densities of $\sim 1 \text{ cm}^{-3}$, ever since the discovery of diffuse H^+ , O stars have been considered the prime candidate for the ionization. Other known energy sources simply fall short in total power (see, e.g., Reynolds, 1984). A key observational step that connected the diffuse ionized gas to radiation from O stars was carried out by Ferguson *et al.* (1996), who showed a quantitative relationship between the DIG and the surface brightness distribution of the bright, O star H II regions across a galactic disk. An example of their work is given in Fig. 8 [their Fig. 4(a)], where it is clear that the mean radial surface brightness profile of the DIG in $H\alpha$ emission tracks that of the H II regions. Their study included a careful, quantitative comparison of the energetic requirements for the $H\alpha$ emission in the DIG with the ionizing radiation and the mechanical energy inferred to be emitted by the O stars in the H II regions of the two galaxies measured. They found that the mechanical energy clearly fell short, by more than a factor of 3. They also found that the maximum contribution of local sources of ionizing radiation in the DIG from stars cooler than spectral type O8 also fell short of the luminosity required, but by a smaller factor. They concluded that the O star populations of the clusters producing the H II regions are the likeliest main source of the radiation that ionizes the DIG.

To test the hypothesis that escaping Lyman continuum photons from the classical H II regions surrounding O

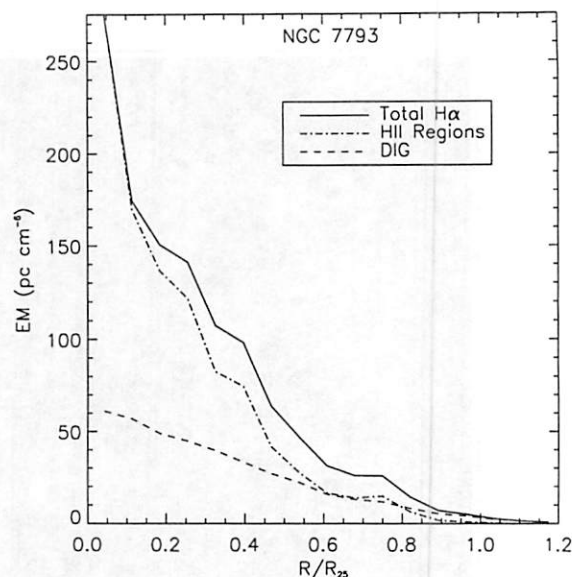


FIG. 8. Deprojected profiles of the (solid) total $H\alpha$ surface brightness into (dash-dotted) H II region and (dashed) DIG emission for NGC 7793. From Ferguson *et al.*, 1996.

stars can be sufficient to ionize the DIG, Zurita *et al.* (2000, 2002) took another important step forward by identifying and classifying the H II regions in a set of photometric maps of disk galaxies in $H\alpha$. This process is illustrated in Fig. 9, taken from Zurita *et al.* (2000), which shows in the upper left, the original continuum-subtracted $H\alpha$ image of the nearly face-on spiral galaxy NGC 157, followed clockwise by a schematic representation of the positions and luminosities of the classified H II regions, a surface brightness map of the DIG in $H\alpha$, with the H II regions subtracted off, and finally a map used for quantifying the DIG. In the case of this last frame, the DIG is measured by integrating the $H\alpha$ surface brightness over the full disk, using the values outside the H II region boundaries and local mean values inside each H II region. Some key points in the method for deriving these maps and quantifying the DIG emission include the following. First a catalog of H II regions was prepared, using a semiautomatic, but interactive method to measure their $H\alpha$ luminosities, effective radii, and central positions (Rozas *et al.*, 1999), down to a lower limiting luminosity. These H II regions were delimited and their emission subtracted from the total image by masking those pixels occupied by the H II regions, but with a final refinement that contiguous pixels with surface brightness higher than a set limit are also subtracted off.

This procedure is illustrated in Fig. 10 (Zurita *et al.*, 2000), which shows how this criterion for separating the H II region from DIG emission coincides well with an alternative criterion in which the boundaries of an H II region are defined by a limiting value of surface brightness gradient. Having separated the H II regions, one can then define the total DIG luminosity in one of three ways: (a) integrating the remaining surface luminosity after applying the H II region mask; (b), as in (a) but

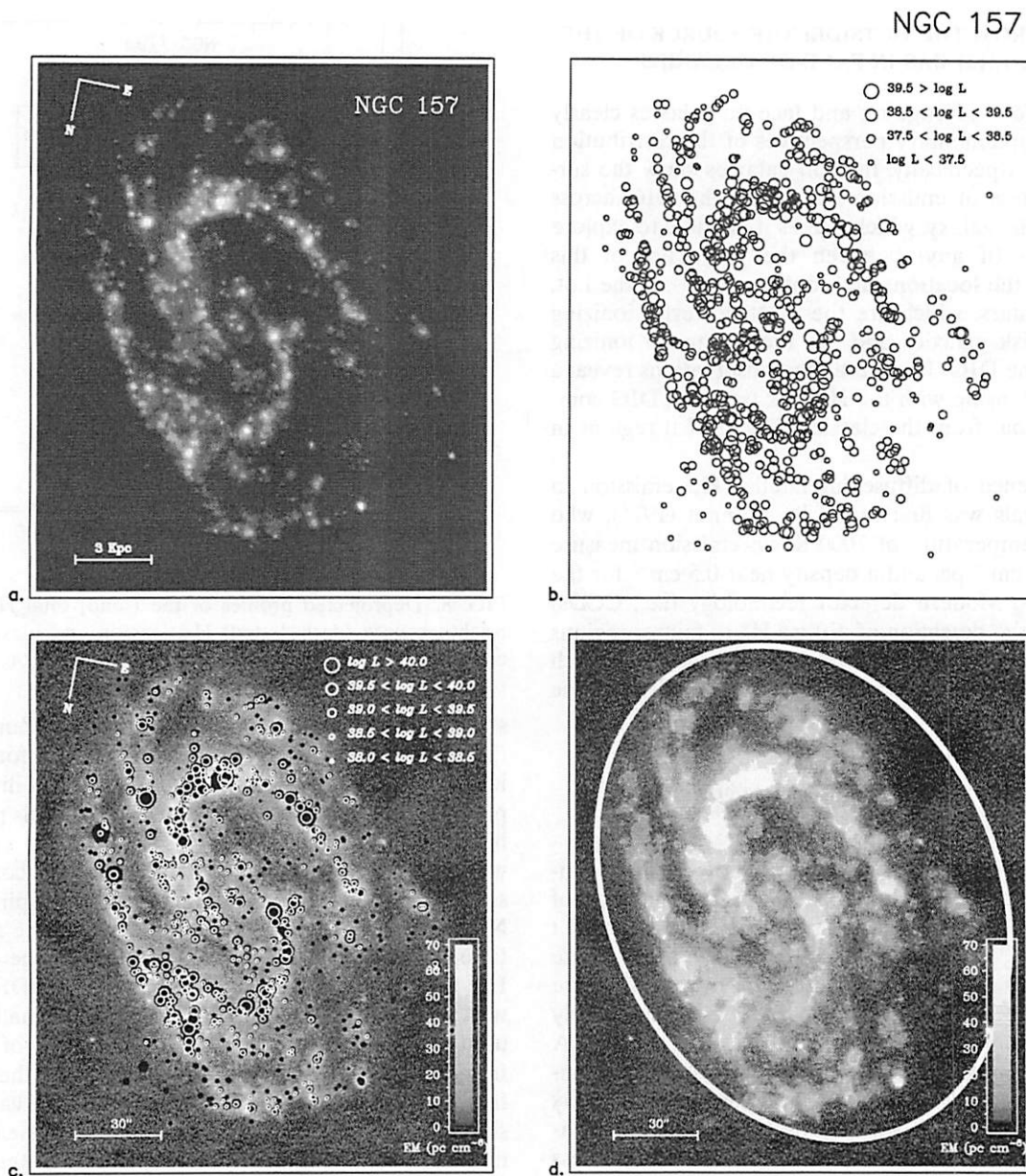


FIG. 9. Steps in the quantification of the total $H\alpha$ luminosity from the DIG for the representative disk galaxy NGC 157. (a) Continuum subtracted $H\alpha$ image. (b) Schematic form of $H\text{ II}$ region catalog, giving position and key to the $H\alpha$ luminosity of each region. (c) Diffuse $H\alpha$ map after subtracting off the catalogued $H\text{ II}$ regions. The brightest $H\text{ II}$ regions are indicated by circles. (d) Measurement of upper limit for DIG. $H\text{ II}$ regions are blanked off, then each is assigned a local value of DIG surface brightness. Ellipse shows limit of integrated DIG flux measured. From Zurita *et al.*, 2000.

then adding a contribution from the areas of the $H\text{ II}$ regions, assuming this is proportional to their projected areas times their local DIG surface brightness; or (c), as in (a) but making the contribution proportional to the area of the $H\text{ II}$ regions times the mean DIG surface brightness outside the regions across the disk of the galaxy. Modes (a), (b), and (c) give, respectively, lower limits, upper limits, and approximate estimates for the total DIG emission from the observed galaxies. In Fig. 11 we show the results of this method of estimating the DIG, for six galaxies, shown as the ratio of the DIG $H\alpha$ luminosity to the total luminosity for the galaxy plotted in terms of galactocentric radius.

We can see that the DIG emits around half of the total $H\alpha$ output, that there are systematic modulations of this tendency with radius, and that there is a slight tendency for the fraction to increase with radius. We also note that the projected area of the disk occupied by the DIG is of order $80(\pm 10)\%$ for all objects shown in Fig. 11. In a separate study of over 100 galaxies, Oey *et al.* (2007) found that the amount of DIG $H\alpha$ to total $H\alpha$ from a galaxy ranged from 20% to nearly 100% with a mean near 60%. Voges (2006) presented results suggesting an inverse correlation between the DIG $H\alpha$ fraction and the star formation rate per unit area.

NGC 157

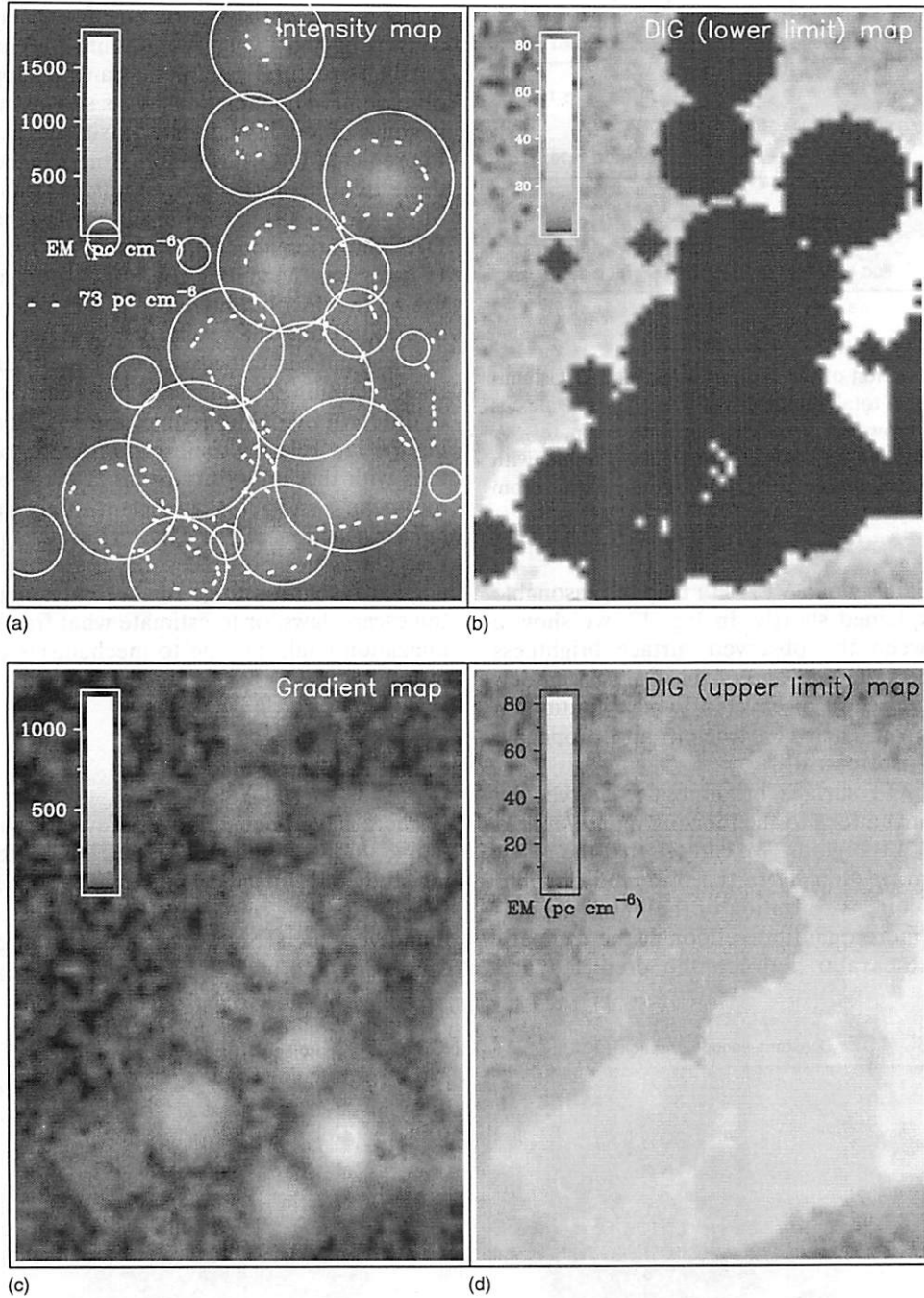


FIG. 10. Technique used for separating H II region emission from DIG emission. (a) Portion of H α image of NGC 157 with crowded field (on a spiral arm). Gray scale in emission measure. Circles show mean catalogued radii of H II regions. Dashed line at 73 pc cm^{-6} , cutoff applied to avoid contamination of DIG by H II regions. (b) Diffuse emission after subtracting off H II regions and applying surface brightness cutoff. (c) Same portion of image in units of H α surface brightness gradient. Applying uniform cutoff at $12.4 \text{ pc cm}^{-3} \text{ pixel}^{-1}$ ($0.28''/\text{pix}$) yields H II region boundaries equal to those found in (a), which confirms this separation technique. (d) Map as in (b), but with H II region mask filled at level of local DIG, giving upper limit case for total galaxy DIG luminosity (see text). From Zurita *et al.*, 2000.

B. An escape model for Lyman continuum propagation

Given a full catalog of H II region positions and luminosities for a galaxy, one can test the hypothesis that

escaping photons from the H II regions cause the ionization of the DIG by modeling the transfer of these photons from their points of origin. This was done by Zurita *et al.* (2002) for NGC 157. This galaxy was selected be-

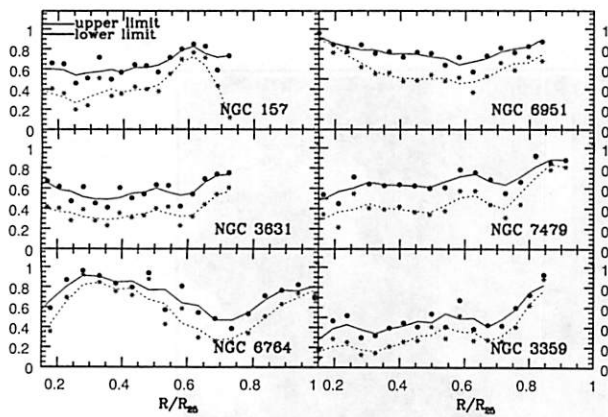


FIG. 11. Radial variation of the ratio of integrated DIG luminosity in $H\alpha$ to the total luminosity for six spiral galaxies (within $0.15R/R_{25}$ crowding precludes accurate estimates). A canonical value for the integrated ratio of $\geq 50\%$ is found, with a total fractional area subtended by the DIG of $\sim 80\%$. From Zurita *et al.*, 2000.

cause of the availability of a VLA H I map of reasonable resolution, as explained shortly. In Fig. 12, we show a comparison between the observed surface brightness distribution in the DIG and one of the simplest models used. In this model, 30% of emitted Lyman continuum photons escape from each H II region, and propagate through the DIG isotropically.

The predicted $H\alpha$ surface brightness is derived by summing the contributions to the ionizing radiation field from each of the H II regions. We can see that the result is remarkably similar globally to the observed distribution, and is itself a fair verification of the initial hypothesis. However, a more quantitative look at the comparison shows that the ratio between the predicted and

observed DIG surface brightness is not uniform on large scales, as would be expected since the initial model assumes a uniform slab structure for the H I involved in converting the Lyman continuum photons to $H\alpha$. The missing structural parameter can be supplied using the observed H I column density, as shown in Fig. 13, where in zones of low H I column density the ratio of observed to predicted DIG surface brightness is reduced. Maps of these two quantities give excellent coincidence of features, and go a step further in showing that the principal DIG ionization sources must be the O stars in luminous H II regions. Modeling the effect of clustered supernovae on the distribution of the H I, Clarke and Oey (2002) also found that the resulting clumpiness of the medium had a significant effect on the escape fraction of the ionizing radiation. Zurita *et al.* (2002) carried out a number of different modeling tests of the basic hypothesis, varying the law relating the escape fraction of ionizing photons with the luminosity of an H II region, and varying the mean absorption coefficient of the inhomogeneous neutral fraction of the DIG. However, they concluded that it was not possible without H I data of improved angular resolution to go further in testing different photon escape laws, or to estimate what fraction of the DIG ionization could be due to mechanisms other than that tested.

C. Line ratio studies

There have been relatively few quantitative spectroscopic studies of the DIG in face-on galaxies. A pioneering study of $[N II]$ and $H\alpha$ across the face of NGC 1068 was carried out by Bland-Hawthorn *et al.* (1991), who found very high $[N II]/H\alpha$ ratios and discussed possible causes for this high excitation. Hoopes and Walterbos

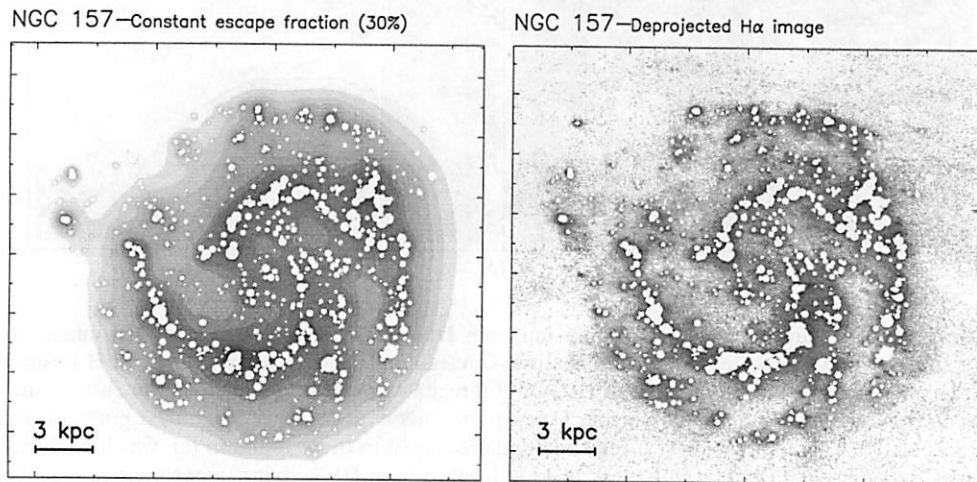


FIG. 12. Comparison of a DIG model with observations. (Left) Modeled surface brightness in $H\alpha$ of the DIG in the disk of NGC 157 assuming 30% of Ly α photons escape from each H II region, and a simple propagation law through a (macroscopically) uniform slab model for the disk. The result is a projection in the plane of the predicted 3D $H\alpha$ column density. (Right) Deprojected image of the galaxy with H II regions masked, and a cutoff of $73 \times \cos i \text{ pc cm}^{-6}$ applied to limit the H II region contamination of the DIG. This shows the basic similarity between these models and the observed DIG, though further refinements are important (see Fig. 13). From Zurita *et al.*, 2002.

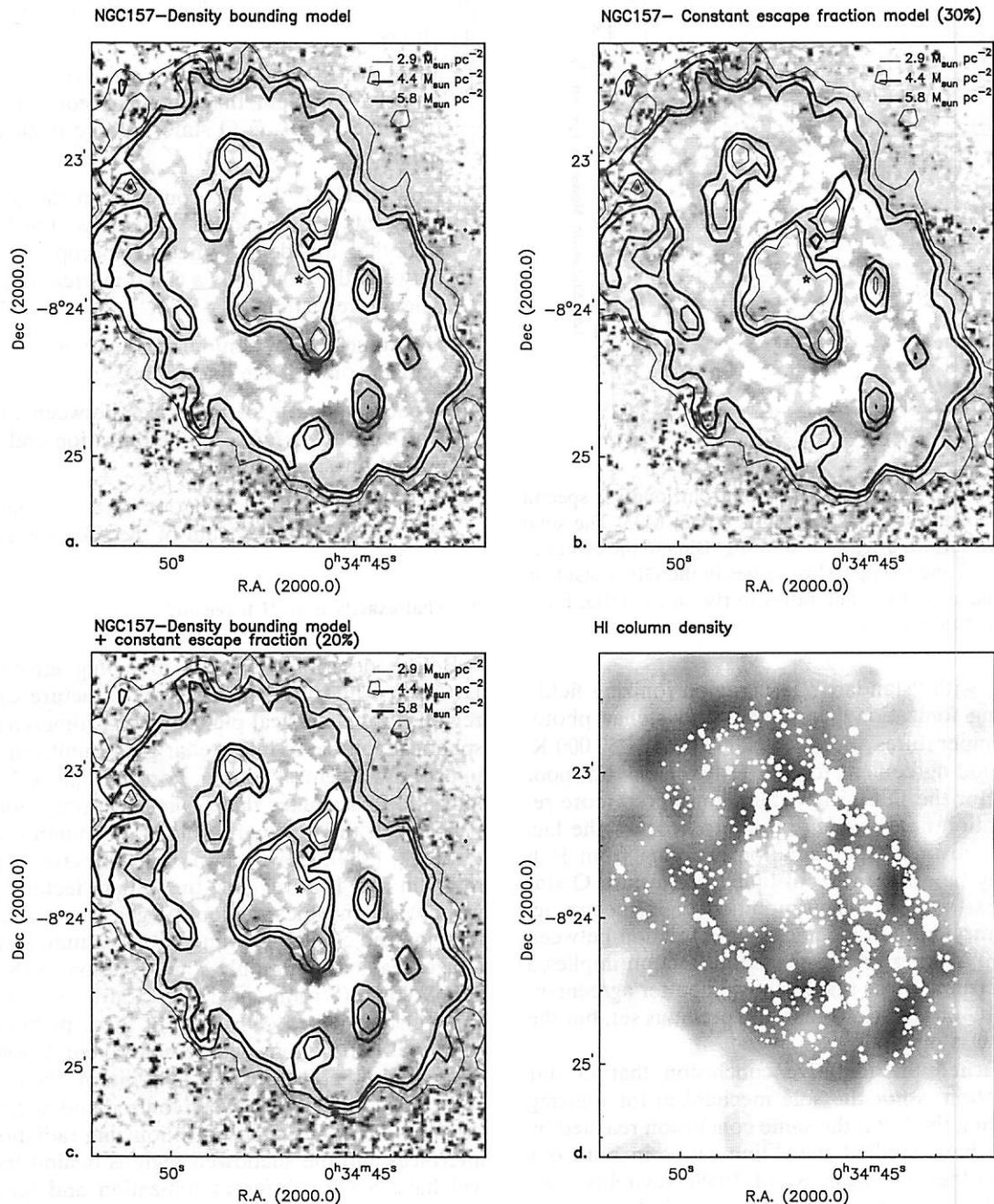


FIG. 13. Ratios of observed to modeled DIG of NGC 157, for three variant models of photon escape from H II regions, assuming a slab structure to the H I in the disk. (a) Constant fraction of photons emitted by the O stars escape from each H II region. (b) Only H II regions with luminosities higher than a critical value show significant Ly α photon escape. (c) A constant underlying escape fraction for all H II regions plus an increasing increment for H II regions above a set H α luminosity. The results are similar for all three. (d) Observed H I column density map (with catalogued H II regions overlaid in black). Note complete coincidence of low zones of observed/modeled ratio with zones of low H I column density, as predicted if photon escape from the H II regions is the main ionizer of the DIG. From Zurita *et al.*, 2002.

(2003) and Voges and Walterbos (2006) made the most careful and detailed examinations to date. In Fig. 14, we show the observations of the DIG close to the luminous H II region NGC 604 in the nearby spiral M33 (Hoopes and Walterbos, 2003), obtained by placing a slit across the H II region so that it sampled the DIG on either side. This example is representative of their study of the three

local face-on galaxies: M33, M51, and M81. We can see that the line ratios $[\text{N II}]/\text{H}\alpha$, $\text{He I}/\text{H}\alpha$, and $[\text{O III}]/\text{H}\beta$ all tend to show higher values in the DIG. The full study includes measurements of these ratios as well as $[\text{S II}]/\text{H}\alpha$ and $[\text{S II}]/[\text{N II}]$ in H II regions and in the DIG, both in the spiral arms and in the interarm zones in each galaxy. The results were compared with predic-

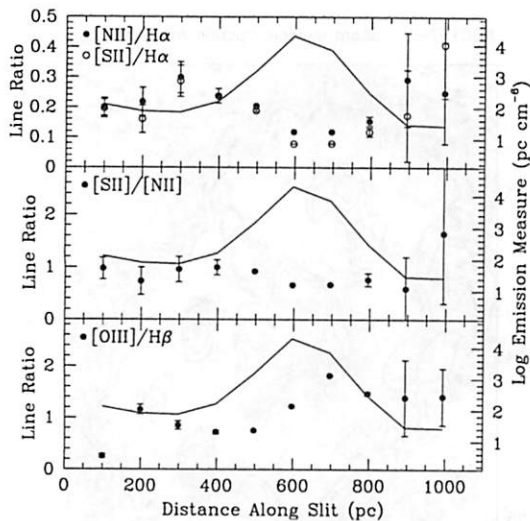


FIG. 14. Selected emission line ratios from long slit spectra across the luminous H II region NGC 604 in M33. The solid line is the H α surface brightness showing rising to the center of the H II region, and falling to low values in the DIG outside it. Note the tendency of the line ratios to rise in the DIG. From Hoopes and Walterbos, 2003.

tions made with “standard” H II region ionizing fields, with varying ionization parameters and stellar photospheric temperatures between 20000 and 50 000 K. There is good agreement for the H II regions but poor agreement for the DIG. They then considered more realistic radiation fields, which take into account the fact that the spectrum of the radiation escaping from H II regions may be different from that from a pure O star (see the next section). They modified their spectra accordingly, varying the modeled escape fraction between 30% and 60%, where a lower escape fraction implies a harder spectrum. These results showed better agreement with the DIG observations than the previous set, but the agreement was only fair.

They reached the tentative conclusion that O star photoionization is not the sole mechanism for ionizing and/or heating the DIG, the same conclusion reached by others who have studied these line ratios in both our Galaxy and others (see, e.g., Rand, 1998; Reynolds *et al.*, 1999; Wood and Mathis, 2004). This may indeed be the case; however, before reaching a definitive conclusion, it would be useful to test a modification of the types of models proposed by Hoopes and Walterbos (2003) based on the assumption that not only is the DIG itself inhomogeneous, but so also the H II regions. The effects of clumping of the interstellar gas on the escape fraction and the spectrum of the ionizing radiation is discussed below.

V. MODELING THE WIM/DIG: EFFECTS OF RADIATION TRANSFER THROUGH A CLUMPY INTERSTELLAR MEDIUM

Models of a more realistic (i.e., 3D clumpy) medium may provide a clearer view of the ionization and heating

processes in the gas as well as insight into the following questions:

- What are the constraints on the structure of the interstellar medium that allow photons to penetrate from the midplane O stars to large distances in the halo?
- How much of the H α comes from the ionized surfaces of dense clouds and how much from a smoother low-density medium occupying the space between the clouds? Is a cloud-intercloud model sufficiently realistic?
- How much extra, nonionizing heating is necessary to explain some of the line ratios?
- What is the role of interfaces between the ionized and neutral gas? Are photoionization codes missing crucial physics at interfaces?
- How much ionizing radiation escapes from galaxies, and what is the spectrum of the escaping radiation?

A. What exactly is an H II region?

Before describing various modeling efforts for the DIG, we will try to envision the structure of an H II region. In the classical picture of a Strömgren sphere, a spherical volume of interstellar gas of uniform density is ionized by a central source. For plausible values of the ionization parameter there is a sharp transition from H II to H I at the Strömgren radius (Strömgren 1939; Osterbrock, 1989). However, in order to better explain line ratios in real H II regions, the “filling factor” approach was devised in which the ionized gas is confined to small, fully ionized clouds surrounded by vacuum, and with the ionized gas occupying only some fraction of the H II region volume (Strömgren, 1948; Osterbrock and Flather, 1959; Osterbrock, 1989). Both of these pictures deviate from real H II regions, where neutral condensations can exist within the H II region. In addition, there may be a convoluted interface between ionized and neutral gas on the faces of clouds exposed to ionizing radiation. These interfaces and the shadowed regions behind the clumps will have a very different ionization and temperature structure and hence also a different emission line spectrum compared to fully ionized clouds or the gas inside a uniform Strömgren sphere (see, e.g., Williams, 1992). Therefore, a more realistic picture of an H II region comprises high-density clumps embedded in a lower-density interclump gas.

Depending on the density of the clumps, they may be fully ionized or be dense enough so that they have an ionized skin and a shielded, neutral interior (see, e.g., Giammanco *et al.*, 2004). This more complex picture can explain qualitatively the observed features of H II regions including “blister” regions such as the Orion Nebula (see, e.g., Ferland, 2001). Consequences of this clumpy structure for emission line ratios from H II regions were quantified by Giammanco *et al.* (2004, 2005). Based on these models, Fig. 15 shows an example of two

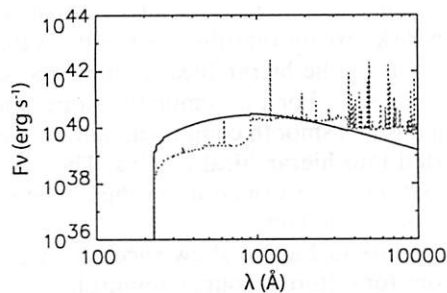


FIG. 15. Components of unattenuated and hardened ionizing spectra emerging from a clumpy model H II region, with geometrical filling factor of denser clumps 10^{-2} , clump density 100 cm^{-3} , and mean clump radius 1 pc. Solid line: Input spectrum emerging diluted but unchanged in relative intensities through interclump medium. Dashed line: Hardened spectrum after transiting internal clumps. In this model, the DIG would be ionized by a combination of both spectra, weighted according to the details of the clump model. For details of these models, see Giammanco *et al.*, 2004.

spectra of ionizing photons emerging from an H II region, one hardened by partial ionization of H I while propagating through the denser clumps within the region, and the other essentially unaffected as it has passed through the interclump gas. Applications to the DIG will entail the combination of these two types of spectra with suitable weightings. When this has been done, we will be in a position to make clearer statements about what fraction of the ionization and heating of the DIG can be due to photons escaping from H II regions, the presumed primary source of the ionization.

B. Modeling the ionization structure of the DIG

A complex 3D picture is almost certainly needed to explain the DIG. As we will see below, a 3D medium can help to answer questions regarding the penetration of ionizing photons to large distances. However, among the most crucial parts of any 3D photoionization model are the density distributions of its gaseous components. If, for example, we adopt a model consisting of dense H I clouds within a uniform lower-density intercloud H I medium, then we will need to know what is the density of the intercloud medium, how much does it contribute to the observed $H\alpha$, and what is the covering factor of the clouds? In models with more complex density distributions, we would need more accurate knowledge about the actual spatial and density distributions of the ionized as well as the neutral gas, which are only beginning to be explored (see, e.g., Hill *et al.*, 2008; Kim *et al.*, 2008). Questions pertaining to the density structure of the interstellar medium are the major unknowns in photoionization models.

Until recently, multidimensional photoionization models of the DIG did not consider the faint forbidden line emission, and focused mostly on $H\alpha$ and the 3D ionization structure of hydrogen via “Strömgren volume” techniques (Franco *et al.*, 1990; Miller and Cox,

1993; Dove and Shull, 1994; Dove *et al.*, 2000) or Monte Carlo simulations (Wood and Loeb, 2000; Ciardi *et al.*, 2002). These models demonstrated that extended DIG layers could be produced by the ionizing radiation of O stars in a clumpy medium, where the 3D density structure of the medium was simulated using a variety of models including “standard clouds” (Miller and Cox, 1993), superbubbles formed by the action of supernovae and stellar winds (Dove *et al.*, 2000), and two-phase and fractal densities (Wood and Loeb, 2000; Ciardi *et al.*, 2002). A 3D density structure was found to be necessary to allow ionizing photons to penetrate to large distances from the O stars, which are confined to discrete locations near the galactic midplane. In a smooth medium with a typical interstellar density of 1 cm^{-3} , an O star will form a Strömgren sphere of radius about 60 pc, and within the neutral medium an ionizing photon will penetrate only 0.1 pc; so, 3D structures must provide the low-density paths that allow the photons to traverse kiloparsec-sized scales and ionize the gas far from the O stars and at large heights above the midplane.

1. Escape of ionizing radiation through superbubbles

Dove *et al.* (2000) investigated whether superbubbles created by the dynamical action of supernovae and stellar winds could provide the low-density paths. They found that the dense swept-up shell of material would trap ionizing photons within the bubble and thus inhibit the escape of ionizing radiation to the halo, unless, of course, the size of the bubble was so large that it reached into the halo. Their models employed a smooth, continuous structure for the swept-up shell. The fragmentation of shells and the punching of holes by supernovae and stellar winds as they expand into a clumpy medium may offset the trapping of radiation in smooth models and allow a larger fraction of ionizing photons to escape. Recent analysis by Terebey *et al.* (2003) of the W4 chimney suggests that a significant fraction of ionizing radiation is able to escape from a fragmented shell-like structure near the midplane, perhaps to be absorbed on the distant wall of a much larger cavity that reaches into the lower halo (Reynolds, Sterling, and Haffner, 2001). Photoionization models of bubbles created by stellar winds in a turbulent star forming cloud also suggest that large escape fractions (in excess of 20%) are possible (Dale *et al.*, 2005). Future work should study the ionization structure of 3D hydrodynamic simulations of supernova created bubbles and superbubbles to determine escape fractions and the spectrum of the escaping ionizing radiation. A comparison of such models with observations of H II regions and the surrounding DIG would allow a critical test of the predicted interstellar structure.

2. Two- and three-dimensional ionization structure of the DIG

The Miller and Cox (1993) model of the DIG adopted a two-component, vertically stratified density structure $n(\text{H}) = 0.1 \exp(-|z|/0.3) + 0.025 \exp(-|z|/0.9)$, where the number density is per cm^3 and the z distance is in kilo-

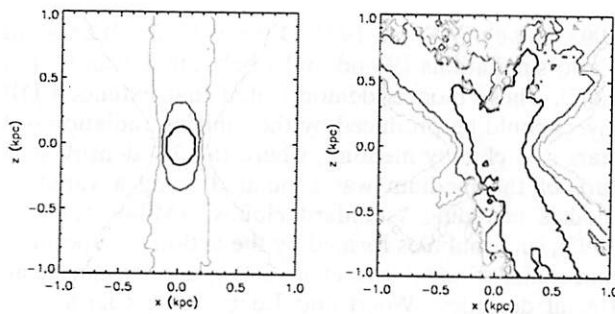


FIG. 16. (Color online) Slices through the ionization structure for point sources in (left) smooth and (right) hierarchically clumped density distributions. The mean vertical density structure for each simulation is that of a Dickey-Lockman disk. From the inner to outer contours, the source luminosities (photons per second) are 10^{49} , 3×10^{49} , 5×10^{49} , and 10^{50} . Comparing the contours in the smooth and clumpy models, it is clear that the 3D density structure provides low-density paths allowing photons to reach much larger distances from the ionizing source.

parsecs. This represents the concentrated neutral layer and the extended ionized layer. They also included an approximation for absorption by dense opaque clouds using a model that reproduces the statistics of clouds in the interstellar medium. Although their smooth density is lower than the average density inferred for H^0 and H^+ , when implemented in their standard cloud model including the known ionizing sources in the solar neighborhood, it reproduced the average observed emission measures (EM) and dispersion measures (DM).

An obvious criticism of the Miller and Cox model is that the mean density they used is smaller than that inferred for the H I in the Galaxy (see, e.g., Dickey and Lockman, 1990). However, they did use the known distribution and ionizing luminosity of O stars in the solar neighborhood and showed that the above density distribution would allow for the gas to be ionized to large $|z|$. In reality the gas is clumped on a wide range of size scales, so the Miller and Cox density provides an estimate of the maximum amount of smooth component allowed, if ionizing photons are to penetrate to large $|z|$. Therefore, the Miller and Cox density profile may be a good starting point for the smooth intercloud medium in 3D models that incorporate both smooth and clumpy components.

To illustrate the effect of a clumpy, 3D density distribution, Fig. 16 shows slices through the ionized volumes created in a completely smooth medium and in a medium with both clumpy and smooth components. In each case to simulate an O star, the ionizing source is a 40 000 K blackbody point source at the center of a grid that is 2000 pc on a side. The hydrogen ionizing luminosity Q is varied in the range $10^{49} < Q < 10^{50} \text{ s}^{-1}$, thus giving a range of sizes for the ionized volumes, corresponding to that for a single O star up to that for a large O star association. For the smooth medium, the density structure is that of a Dickey-Lockman disk (Dickey and Lockman, 1990). For the clumpy medium, the average

$|z|$ -height-dependent density is also that of a Dickey-Lockman disk, except that the gas has been turned into 3D clumps using the hierarchical clumping algorithm of Elmegreen (1997). For this simulation, one-third of the mass remains in a smooth component and the remainder is converted into hierarchical clumps. The photoionization simulation is performed using the 3D Monte Carlo code of Wood *et al.* (2004).

The contours in Fig. 16 show slices through the ionized regions for different source luminosities. It is immediately seen that for a given source strength the 3D density structure with clumps allows ionizing photons to reach much larger $|z|$ distances than the completely smooth distribution. In the smooth model, the source with $Q = 10^{49} \text{ s}^{-1}$ (typical of a single O star) creates a very small ionized volume, while the same source ionizes a much larger volume in the 3D simulation. Recall that both the smooth and clumpy density grids have the same mean $n(z)$ given by the Dickey-Lockman density distribution. Therefore, it appears that 3D density structure readily allows for ionizing photons to penetrate to large $|z|$, thus solving a problem common to models that adopt a smooth density structure of the medium.

C. Modeling the emission line spectrum of diffuse ionized gas

The physical conditions in the DIG are revealed through its emission line spectrum, which probes its ionization state and temperature structure (Sec. II). The main observational characteristics that successful models of the DIG spectrum must address are as follows:

- The temperature, probed via the dominant ion ratios $[N \text{ II}]/H\alpha$ and $[O \text{ II}]/H\alpha$, appears to rise with increasing $|z|$ height above the plane. Most of the nitrogen and oxygen are N^+ and O^+ , and $[N \text{ II}]$ and $[O \text{ II}]$, excited by electron collisions, are very sensitive to temperature.
- Compared to traditional H II regions, the DIG appears to be ionized by a softer radiation field. This is revealed in the elevated $[S \text{ II}]/[N \text{ II}]$, a measure of S^+/S , and the apparent underionization of He implied by low $He \text{ I}/H\alpha$ recombination line intensity ratios.
- WHAM observations showed that $[O \text{ I}]/H\alpha$ is weak, at least near the galactic midplane, while in NGC 891 $[O \text{ I}]/H\alpha$ is observed to increase with increasing distance above the plane. Models predict that interfaces between the ionized and neutral regions should be revealed by increased $[O \text{ I}]/H\alpha$ and a rapid rise of $[N \text{ II}]/H\alpha$ and $[S \text{ II}]/H\alpha$ near the transition region, where the gas temperature is rising rapidly.
- In some galaxies $[O \text{ III}]/H\alpha$ is seen to remain high or even increase at large $|z|$ heights, whereas photoionization models predict $[O \text{ III}]/H\alpha$ to decrease with height above the plane.

1. One-dimensional models

While the 2D and 3D techniques described above were used to explain the formation and structure of the DIG via O-star photoionization, detailed 1D photoionization codes were used to explain the DIG's emission line spectrum (see, e.g., Mathis, 1986, 2000; Domgorgen and Mathis, 1994; Sembach *et al.*, 2000; Collins and Rand, 2001; Hoopes and Waltherbos, 2003). In general, the 1D simulations parametrized the problem with an ionization parameter, calculated the ionization structure of a constant density spherically symmetric volume, and formed line ratios by taking ratios of the total emission line intensities from the entire volume. By combining simulations with different ionization parameters and different supplemental heating rates, these volume-averaged models could explain many of the observed line ratios in the DIG. However, 1D models do not allow for a self-consistent explanation of the observed trends of line ratios. In particular, $[\text{N II}]/\text{H}\alpha$ and $[\text{S II}]/\text{H}\alpha$ are observed to be anticorrelated with the $\text{H}\alpha$ intensity and increase with increasing distance from the midplane (see, e.g., Rand, 1998; Haffner *et al.*, 1999).

Explaining these observational trends requires models that do not use volume averages, but form line ratios for lines of sight that pierce through the ionized volume at increasing impact parameters away from the ionizing source. The plane parallel slab models presented by Bland-Hawthorn *et al.* (1997) showed how the depth dependence of the ionization and temperature structure (see their Fig. 9) could explain the trends for $[\text{N II}]/\text{H}\alpha$ line ratios with distance from the source. More recently, Elwert and Dettmar (2005) presented a grid of plane parallel models that could explain the observed increase of $[\text{N II}]/\text{H}\alpha$ and $[\text{S II}]/\text{H}\alpha$ above the midplane.

A persistent problem with these photoionization models is that they cannot explain the rise of $[\text{O III}]/\text{H}\alpha$ with height above the plane unless some other ionization and/or heating source is invoked, such as shocks, photoelectric heating, or turbulent mixing layers (Slavin *et al.*, 1993; Reynolds *et al.*, 1999; Collins and Rand, 2001). Also, unless the medium is fully ionized beyond the edge of the simulation (i.e., density bounded), the models predict uncomfortably large $[\text{O I}]/\text{H}\alpha$ ratios at the edge of the ionized volume. Clumping in H II regions may explain the apparent absence of these edge effects as discussed below.

2. Two- and three-dimensional models

Recent advances in the development of Monte Carlo photoionization codes (Och *et al.*, 1998; Ercolano *et al.*, 2003; Wood *et al.*, 2004) now enable calculations of the ionization and temperature structure and emission line strengths for multiple ionizing sources within 3D geometries. Wood and Mathis (2004) presented simulations for photoionization and line intensity maps of a stratified interstellar medium. Their models showed that, due to hardening of the radiation field in the spectral region between the H I and He I ionization edges, the temperature naturally increases away from the ionizing source.

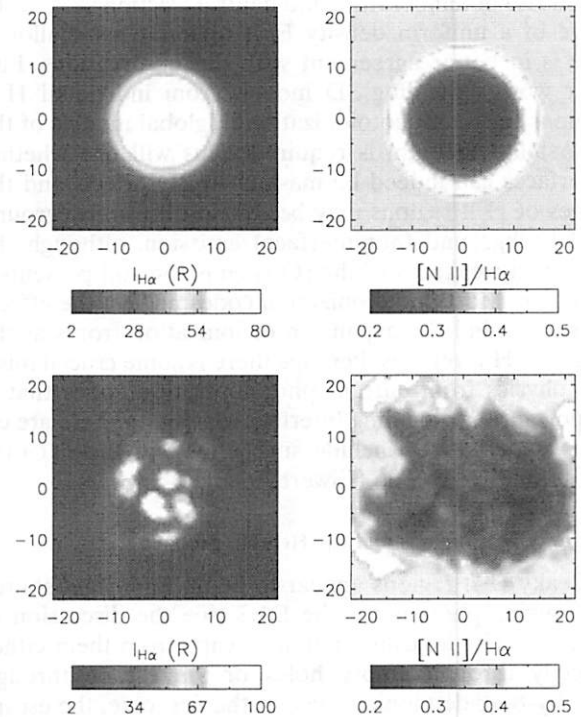


FIG. 17. $\text{H}\alpha$ and $[\text{N II}]/\text{H}\alpha$ maps for (upper panels) uniform density and (lower panels) hierarchically clumped H II region models. In each simulation, a uniform background has been added to the $\text{H}\alpha$ and $[\text{N II}]$ maps to simulate the H II region being surrounded by low-density DIG. Notice the very irregular boundary in the clumpy model and that the rise of $[\text{N II}]/\text{H}\alpha$ with distance from the central source is much steeper in the smooth model.

They also found that $[\text{N II}]/\text{H}\alpha$ and $[\text{S II}]/\text{H}\alpha$ rise with $|z|$ in their vertically stratified density structure and that $[\text{S II}]/[\text{N II}]$ remains fairly constant with $|z|$ as observed. While their models could explain most of the line ratios, additional nonionizing heating was still required to produce the largest line ratios observed.

3. Interfaces and three-dimensional H II regions

In standard photoionization models of the interface between ionized and neutral gas, the medium is turning neutral and the temperature is rising rapidly due to the hardening of the radiation field (see, e.g., Wood and Mathis, 2004). For optical observers, such an interface should be characterized by enhanced emission of $[\text{O I}]$, $[\text{N II}]$, and $[\text{S II}]$ relative to $\text{H}\alpha$. As mentioned above, these effects have in general not been observed in the DIG. However, recent results from the WHAM survey of low emission measure H II regions do appear to show an increase of $[\text{N II}]/\text{H}\alpha$ and $[\text{S II}]/\text{H}\alpha$ away from the ionizing sources (Wood *et al.*, 2005). Figure 17 shows that models of hierarchically clumped H II regions give a shallower rise of $[\text{N II}]/\text{H}\alpha$ away from the ionizing source than that predicted by uniform density models. This is because the edge of the H II region is very irregular and sightlines probe different columns of ionized gas and different temperatures compared to the regular,

rapid rise in temperature and neutral fraction seen at the edge of a uniform density H II region. This shallower rise is in better agreement with the observations. Further work extending 3D models from individual H II regions to study photoionization in global models of the interstellar medium is required. This will test whether interfaces can indeed be masked by 3D effects and the edges of H II regions may be lost in diffuse foreground and background (noninterface) emission, although the observed weakness of the [O I] emission still presents a problem. Most photoionization codes neglect the effects of shocks and the expansion of ionization fronts at the edges of H II regions. Perhaps there is some crucial missing physics from current photoionization codes that is important for modeling interface emission. There are efforts underway to include such effects in the CLOUDY photoionization code (Elwert, 2005).

4. Leaky H II regions and the He⁺/H⁺ problem

Leaky H II regions appear to be an important source of ionizing photons for the DIG (see the discussion in Sec. IV). The ionizing photons escape from them either directly through empty holes or via escape through density-bounded ionized gas. In the first case, the escaping spectrum will be that of the ionizing star, while in the second case the spectrum will be modified due to partial absorption of the radiation by neutral H and He. Compared to the intrinsic stellar spectrum, the escaping spectrum is generally harder in the H-ionizing continuum and has its He-ionizing photons suppressed (see, e.g., Hoopes and Waltherbos, 2003; Wood and Mathis, 2004).

A combination of direct escape and transmission through density-bounded ionized gas is likely to occur in a 3D H II region. In fact, line ratios in the DIG surrounding leaky H II regions may allow us to determine whether the escaping photons are dominated by those escaping through true holes in the H II region or by those penetrating density-bounded H II gas. Specifically, the suppression of He-ionizing photons penetrating density-bounded H II regions may explain the underionization of He in the DIG. However, more observations of He I and other lines as a function of distance from H II regions in our Galaxy and others are required to test this. It cannot yet be ruled out that most of the DIG ionization is produced by later O stars (which have a soft spectrum consistent with the He I observations), because the earliest (hard-spectrum) O stars may preferentially have their ionizing radiation absorbed within their parent molecular clouds. However, a study of face-on galaxies suggests that these cooler O stars do not provide sufficient ionizing power (Ferguson *et al.*, 1996). Clearly more observational and theoretical investigations are required into the role of leaky H II regions and the spectrum of their escaping ionizing radiation.

VI. IONIZING RADIATION FROM HOT-GAS-COOL-GAS INTERFACES

Early-type stars produce a prodigious amount of ionizing radiation and are capable of ionizing gas well

above the midplane of the Galaxy. But does this stellar radiation explain all of the observed H⁺? For example, do some of the O star photons completely escape the Galaxy to account for the ionized gas observed in the high-velocity H I clouds (HVCs) and the Magellanic Stream, located up to 50 000 pc from the Galaxy (Weiner and Williams, 1996; Tufté *et al.*, 1998; Putman *et al.*, 2003)? If so, then the H α surface brightness of these clouds provides a direct measurement of the flux of Lyman continuum radiation that completely escapes the Galaxy (see, e.g., Tufté *et al.*, 1998). However, because these cooler clouds appear to be immersed in a much hotter plasma (see, e.g., Savage *et al.*, 2003), we must at least consider the fact that hot-gas-cool-gas interfaces are also a source of ionizing radiation. Such radiation may even play an important role in the ionization of a very local H I cloud in the vicinity of the Sun.

Observations of O⁵⁺ and detections of other ions in high states of ionization (Sembach and Savage, 1992; Savage *et al.*, 2000; Sembach *et al.*, 2003) show that interfaces between hot ($\sim 10^6$ K) gas and cooler ($\lesssim 10^4$ K) gas are widespread throughout the interstellar medium and galactic halo. The resulting intermediate temperature ($\sim 10^5$ K) gas at these interfaces produces extreme ultraviolet ionizing radiation. Thus, even though O star photons can leak through a clumpy interstellar medium and/or through superbubble chimneys, interfaces have the advantage that they exist wherever the hot gas and cooler clouds do, including places where ionizing radiation from O stars does not reach. Although significantly weaker than the flux from hot stars, interface radiation may be more widely distributed, and because the emission is generated in a thin layer adjacent to the absorbing cloud, interface radiation is efficiently used for ionizing that cloud as well as being a source of ionization for other more distant clouds.

A. Types of interfaces

A variety of different types of interfaces may exist, depending on the physical processes operating and dynamical state of the boundary region between the hot and cooler gas. These include evaporative boundaries (see, e.g., Cowie and McKee, 1977), cooling-condensation fronts (Shapiro and Benjamin, 1991), and turbulent mixing layers (Begelman and Fabian, 1990; Slavin *et al.*, 1993). In evaporative boundaries, thermal conduction heats the cool cloud and produces an outflow. This requires that the magnetic-field topology is such that the warm gas is not shielded too thoroughly from the hot gas. In cooling-condensation fronts, slow accretion of hot gas onto the cool gas occurs as the hot gas cools radiatively. A turbulent mixing layer (TML) can develop in regions where there is shear flow at the hot-cool boundary that leads to hydrodynamical instabilities and mixing of the hot and cool gas. The mixed gas in a TML cools rapidly due to its temperature and nonequilibrium ionization state. Although these types of interfaces share some characteristics, the ionization state of the gas can be radically different for different types

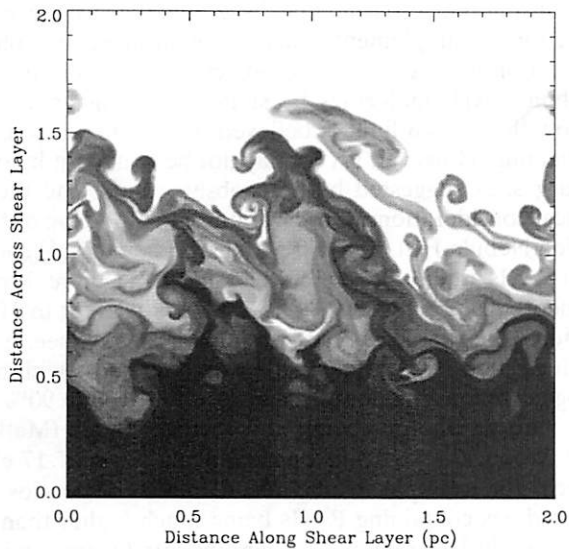


FIG. 18. Temperature in a shear layer between hot and warm gas. The hot gas (top, $T=10^6$ K) flows to the left at 10 km s^{-1} while the warm gas (bottom, $T=8000$ K) flows to the right at 10 km s^{-1} . Cooling is not included in this 2D calculation.

of interfaces. For example, relative to collisional ionization equilibrium, the gas can be highly underionized in evaporative outflows, overionized in cooling-condensation fronts, or a combination of both overionized and underionized as in a TML, wherein the formerly cool gas is underionized and the formerly hot gas is overionized. In Fig. 18, we show the results of preliminary numerical hydrodynamic simulations of a TML. Other possibilities exist for hot-gas-cool-gas interfaces involving various combinations of cooling, conduction, and mixing, but those have yet to be explored.

The flux and spectrum of ionizing radiation emitted is determined by the ionization-temperature-density profile in the interface. In general, underionized gas radiates more strongly than overionized gas, because ions that are being ionized up will generally be excited several times before being ionized. In Fig. 19, we show a comparison of the EUV to soft-x-ray spectrum generated in an example evaporating cloud boundary and

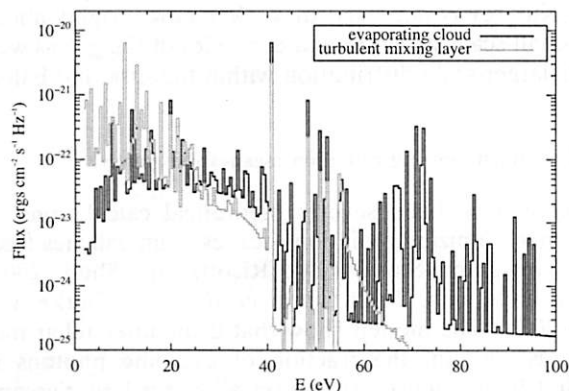


FIG. 19. Comparison of ionizing flux generated in an evaporating cloud with that generated in a turbulent mixing layer.

TML. In this calculation, the hydrogen-ionizing photon production rate between 14 and 24 eV is approximately $2 \times 10^4 \text{ photons cm}^{-2} \text{ s}^{-1}$. This is only about 10% of the ionizing flux that appears to be incident on high-velocity clouds in the galactic halo (see, e.g., Tufté *et al.*, 1998, 2002), for example; however, the uncertainty in the properties and morphology of actual cloud interfaces (the number of interfaces a line of sight through a cloud intersects; see Fig. 18) leaves open the possibility that the $\text{H}\alpha$ produced by interface radiation could be significant in regions where stellar ionizing photons do not reach.

B. A test case

The local interstellar cloud (LIC) that surrounds the Solar System appears to be an excellent candidate for exploring interstellar interfaces. It is inside the local bubble (Cox and Reynolds, 1987), and thus probably surrounded by hot gas. There is no direct Lyman continuum radiation from O stars and the nearest B star (ϵ CMA) is more than 100 pc away. The ionization of the LIC is very well characterized (it is the best observed interstellar cloud in the Universe), and its ionization state is somewhat unexpected, that is, quite different from the WIM. In the LIC, hydrogen is only moderately ionized at $\sim 20\text{--}40\%$, and He is more ionized than H.

Models that include ionizing radiation from an evaporative interface (Slavin and Frisch, 2002; Frisch and Slavin, 2003) are generally successful in matching the myriad of data available and indicate that a diffuse EUV source above the weak ionizing flux provided by nearby stars is necessary to explain the ionization. Problems remain, however, in explaining the relatively low column densities of O^{5+} and C^{3+} as well as the high column of Si^{2+} that have been observed (Gry and Jenkins, 2001; Oegerle *et al.*, 2005). These discrepancies would seem to point to a different type of interface surrounding the LIC. The existence of the LIC does raise the question of how common such partially ionized clouds are and how much they contribute to the diffuse interstellar H^+ (see, e.g., Reynolds, 2004). While the density and temperature of the LIC are very close to what is found in the WIM, the low values of $[\text{O I}]/\text{H}\alpha$ observed by WHAM imply that H^+/H for most of the diffuse ionized gas in the solar neighborhood is much closer to unity than the lower value found for the LIC (although He^+/He may be similar).

In summary, while many aspects of the physics of interfaces are yet to be explored, the fluxes produced by such interfaces are probably weaker than the ionizing fluxes require to produce the WIM (Sec. II). Also, the ionization state of the LIC cloud suggests that such clouds can account for only a small portion of the ionization associated with the WIM. Nonetheless, there are several conclusions we can draw from existing observations and theory that are relevant to the WIM:

- (1) Hot-cool gas interfaces appear to be widespread through the interstellar medium. Wherever inter-

faces with intermediate temperature gas ($T \sim 10^5$ – $10^{5.5}$ K) exist, there will be ionizing radiation generated, producing diffuse ionization. The fact that the spectra peak in the EUV and that a large fraction of the generated flux should be captured by the cool cloud gas makes interface radiation a potentially significant source of ionizing radiation in regions shielded from direct O-star Lyman continuum photons. For example, if the interface is very convoluted, a typical line of sight through a cloud may pass through many hot-cool surfaces, resulting in a total $H\alpha$ intensity for the cloud that is comparable to what is observed for the HVCs. Interface radiation appears to be required to explain the properties of the local cloud near the Sun.

- (2) The theoretical spectra from evaporating clouds and turbulent mixing layers are harder than that of the O stars, which could result in the presence of some ions in the WIM that O stars cannot produce.
- (3) The type of interface that exists at the boundary of a cloud depends (at least) on the dynamics of the boundary, the geometry of the cloud, and the degree to which thermal conduction occurs. Thus refinements in theory and observations of good candidate clouds are needed to determine the extent to which interfaces contribute to ionization in our Galaxy and others.

VII. SOME QUESTIONS FOR FUTURE STUDY

A. What is the source of the elevated temperatures?

Some of the line ratios, including $[O\ III]/H\alpha$ and the largest observed $[N\ II]/H\alpha$ and $[S\ II]/H\alpha$ ratios, do not seem to be explained by photoionization, even when hardening of the O star's radiation is considered (Sec. V). Do shocks play a role (Collins and Rand, 2001; Hidalgo-Gómez, 2005)? Or is there some additional source of nonionizing heat, such as photoelectric heating from interstellar dust particles or large molecules (Reynolds and Cox, 1992; Weingartner and Draine, 2001), dissipation of turbulence (Minter and Spangler, 1997), magnetic reconnection (Raymond, 1992), and shocks and cooling hot gas (Slavin *et al.*, 1993; Collins and Rand, 2001)? Most of these mechanisms seem capable of generating heating rates of the order 10^{-26} erg s^{-1} cm^{-3} , the power requirement for the additional heat source [see the discussion in Reynolds *et al.* (1999)]. In addition, Reynolds *et al.* (1999) showed that for these nonionizing sources their heat can dominate over that from photoionization at low ($\lesssim 10^{-1}$ cm^{-3}) densities, because their heating rates are proportional to the first power (or less) of the density, rather than the second power as with photoionization. This could explain the observed inverse correlation between the line ratios and the $H\alpha$ intensity (see Fig. 2). Ways of discriminating between these mechanisms are very much needed, but none is yet forthcoming.

Can photoelectric heating be eliminated as a candidate for the supplemental heat? In neutral gas, the photoejection of electrons from polycyclic aromatic hydrocarbon (PAH) molecules by stellar ultraviolet photons below the Lyman limit is believed to be a major source of heating. However, PAHs may not be abundant in ionized gas, as suggested by both observational and theoretical considerations. Observations and modeling of the Orion Nebula H II region (see, e.g., Ferland, 2001) show that PAHs are not present in the ionized gas there. From a theoretical perspective, if PAHs were present in H II regions, their large Lyman continuum opacity (see, e.g., Weingartner and Draine, 2001) would compete with hydrogen for ionizing photons and result in around 90% of the ionizing photons being absorbed by PAHs (Mathis and Wood, 2005). PAH opacity peaks around 17 eV, which, for example, would result in He^+/H^+ ratios in ionized gas containing PAHs being much higher than is observed in H II regions surrounding late O stars and in the DIG. On the other hand, siliceous dust particles have a grayer wavelength-dependent opacity and only absorb about 5% of ionizing photons in the Mathis and Wood (2005) simulations, not significantly changing the He^+ abundance or other line ratios. However, the role they may play in photoelectric heating is unclear.

B. What is the spatial distribution of the gas?

Does the widespread $H\alpha$ emission originate from a low-density intercloud gas that occupies large volumes of the interstellar medium? Or is some significant fraction of the $H\alpha$ coming from the denser ionized faces of clouds or superbubble walls? Models investigating the different scenarios and comparisons of the resulting emission line and line ratio maps with observations, including electron column densities from pulsar dispersion measures, may provide some answers. Hill *et al.* (2008) showed that the statistical distribution of emission measures in the WIM is well matched by the density distribution produced in magnetohydrodynamic (MHD) models of an isothermal, mildly supersonic turbulent medium. Also, new observational methods that sample the H^+ at very small scales (Hill *et al.*, 2003) or that access emission lines in a different spectral region (see, e.g., Kutyrev *et al.*, 2004) may offer new insights about the small-scale structure and dynamics of the gas as well as its larger-scale distribution within the disk and halo.

C. How much ionizing radiation escapes the galaxy?

There have been several theoretical calculations of how much ionizing radiation escapes from galaxies (see, e.g., Dove and Shull, 1994; Ricotti and Shull, 2000; Wood and Loeb, 2000; Ciardi *et al.*, 2002; Clarke and Oey, 2002). The models show that if the interstellar medium is smooth, the fraction of escaping photons is small. Clumpy density structures allow for larger escape fractions through low-density paths in the interstellar medium (see Fig. 16). However, there are few observa-

tions to test these models and determine how much ionizing radiation actually escapes. If interface radiation or shocks (Bland-Hawthorn *et al.*, 2007) are not a major source of ionization, then one promising avenue is to study the ionized surfaces of distant high-velocity clouds surrounding the Galaxy (Tufté *et al.*, 1998, 2002). Tufté *et al.* (1998), Bland-Hawthorn and Maloney (1999), and Putman *et al.* (2003) estimated that a few percent of the ionizing luminosity from the Galaxy would be required to explain the H α emission from high-velocity clouds located $\sim 10\,000$ pc above the disk (Wakker, 2004). As discussed in Sec. V, the spectrum of the escaping radiation (e.g., from future observations of He I/H α from intermediate and high-velocity clouds) could reveal whether photons escape the galaxy through very low-density channels or by filtering through density-bounded ionized regions.

D. Do hot, pre-white dwarf stars play a role?

In their late stages of evolution, low-mass stars pass through a hot photospheric phase after shedding their outer envelopes. Once the stellar envelope (i.e., the planetary nebula) has expanded sufficiently and is optically thin to the ionizing radiation from the stellar core, the Lyman continuum photons are available to ionize the ambient interstellar medium. Such stars may be responsible for the ionization of small, localized regions in the low-density interstellar medium (Reynolds *et al.*, 2005), but it is not known whether they also contribute significantly to the more diffuse ionizing radiation producing the WIM. Their luminosities and their lifetimes in this phase are orders of magnitude smaller than that of massive O stars; however, in comparison to O stars, their numbers are enormous, and they are much more uniformly distributed throughout the Galactic disk. Early calculations by Hills (1972) indicated that the ionizing radiation from these hot pre-white dwarf stars could significantly influence the interstellar medium. Since then, there has been progress in understanding the late stages of evolution of low mass stars, but little additional work has been carried out on their collective, large-scale influence on the interstellar medium.

E. Are missing atomic data important?

Presently photoionization models are unable to make accurate predictions of the [S II] emission from the DIG because the dielectronic recombination rates for sulfur are unknown [see the discussion in Ali *et al.* (1991)]. The determination of these rates is important because they impact the inferred S⁺ and S²⁺ abundances in the DIG, and because sulfur is an important coolant, influencing the predicted strengths of other lines. While efforts are underway to calculate these dielectronic recombination rates, there may also be a handle on the rates observationally via modeling the emission line strengths for large, low surface brightness H II regions.

F. What insights will new global models provide?

A next step in modeling would be to test global dynamical models of the interstellar medium (see, e.g., de Avillez and Berry, 2001; Kowal *et al.*, 2007) to see whether their density structures can allow for O star radiation to produce the observed ionization (H α emission) and temperature structure (line ratios) of the DIG. This will be a formidable task, combining large-scale 3D dynamical and radiation transfer simulations. A unique solution for the structure of the interstellar medium may not even be possible without also incorporating observations of the other gas phases. However, combining dynamical and photoionization models would provide observational signatures that could be searched for. Perhaps progress could be made in testing various scenarios—ruling out classes of models, determining what conditions (density and dynamics) are required to allow radiation to escape to the halo, and determining which models best fit the observed distribution and kinematics of the H α over the sky.

While much progress has been made in understanding the nature of the warm ionized medium and the basic physical processes occurring within it, the future promises to be a very exciting time, when the advances in computing ability are combined with high spatial and spectral resolution observations of this gas and other major phases of the interstellar medium. There is much still to be learned.

LIST OF ACRONYMS AND TERMS

Chimney	a superbubble that extends from the galactic midplane, where it has been energized by supernovae, into the halo. Chimneys can be a conduit for hot gas and hydrogen-ionizing radiation.
DIG	diffuse ionized gas characterized by temperatures $\sim 10^4$ K and densities $\sim 10^{-1}$ cm ⁻³ that occupies the disk and halo of many spiral galaxies. In our Galaxy, the DIG is often referred to as the warm ionized medium (WIM).
DM	dispersion measure; the free-electron density integrated along the line of sight to a pulsar; $\int_0^P n_e ds$. Because the free-electron density $n_e \approx n_{H^+}$ in the interstellar medium, DM is essentially the column density of the H ⁺ .
EM	emission measure; the product of the proton density times the electron density integrated along the line of sight. In regions of nearly fully ionized hydrogen, emission measure is essentially $\int n_e^2 ds$.
EPIC	European Photon Imaging Cameras on the XMM-Newton's x-ray telescopes.
FIR	far infrared (wavelengths $\sim 10^2$ μ m).
Forbidden line	an emission line produced by the decay of an excited metastable state in an

	atom or ion, denoted by square brackets around the ion's symbol. In the low-density WIM/DIG, the collisional deexcitation time scales are much longer than the radiative decay time scales, and therefore the intensity of a forbidden line measures the excitation rate of the metastable state due to collisions by the thermal electrons in the plasma.		
The Galaxy	with a capital "G," our galaxy, the Milky Way.	SFR	star formation rate.
Galactic latitude	the angular distance above the Galactic equator, the midplane of the Milky Way.	Spiral galaxy	a galaxy that has a flat, rotating disk of stars, gas, and dust.
H α	the emission at 6563 Å produced by the hydrogen Balmer-alpha ($n=3 \rightarrow 2$) transition following the recombination of ionized hydrogen.	Superbubble	a large cavity of hot ($\sim 10^6$ K), ionized gas created by the combined kinetic energy of multiple supernovae occurring within an active star formation region.
H I region	a cloud composed primarily of neutral hydrogen atoms.	T_e, T_i	electron temperature and ion temperature, respectively. In general, $T_e = T_i$ in the interstellar medium.
H II region	a discrete region of photoionized hydrogen associated with a hot star; a classical "emission nebula" or "Strömgren sphere," as opposed to the more widespread, lower density H $^+$ (the WIM, DIG) not clearly associated with a single, discrete source of ionization.	TML	turbulent mixing layer; the transition region between two adjacent parts of the interstellar medium that have very different temperatures and are moving with respect to each other.
H $^+$	ionized hydrogen; in this paper ionized hydrogen associated with the widespread, low-density WIM/DIG.	VLA	the Very Large Array radio synthesis telescope near Socorro, New Mexico.
HST	the Hubble Space Telescope.	WHAM	the Wisconsin H-Alpha Mapper; a remotely controlled observatory dedicated to the detection and study of faint emission lines from the interstellar medium of the Galaxy.
HVC	high velocity cloud; a neutral hydrogen cloud, usually located far from the galactic disk and not partaking in the rotation of the disk.	WIM	the widespread, warm, ionized medium in the Galaxy characterized by temperatures $\sim 10^4$ K and densities $\sim 10^{-1}$ cm $^{-3}$; sometimes also called the "Reynolds layer."
Ionization parameter	the ratio of the ionizing photon density to the electron density, which, along with the spectrum, determines the population of ionization states in photoionized gas.	WNM	widespread neutral atomic hydrogen characterized by temperatures $\sim 10^3$ K and densities $\sim 10^{-1}$ cm $^{-3}$.
LIC	the very local interstellar cloud within a few parsecs of the Sun.	XMM-Newton	the Multi-Mirror Mission orbiting x-ray observatory of the European Space Agency.
LyC	Lyman continuum; energies above the Lyman limit, the ionization potential of hydrogen (13.6 eV).	z	the perpendicular distance from the midplane of a spiral galaxy.
Magellanic Stream	an extended complex of neutral atomic hydrogen gas associated with a pair of satellite galaxies, the large and small Magellanic clouds, orbiting the Galaxy.		
O and B stars	hot stars that emit Lyman continuum (LyC) photons. Massive O stars are located in active star forming regions, emit a large fraction of their luminosity in the LyC, and are believed to be the primary source of ionization for the WIM/DIG.		
PAH	polycyclic aromatic hydrocarbon; a large interstellar molecule that can inject heat into the interstellar via its ionization by ultraviolet photons from stars.		

ACKNOWLEDGMENTS

We thank Carl Heiles for his contributions, enthusiasm, encouragement, and insights over the years. We also thank the meeting organizers, Y.-H. Chu and T. Troland, without whom this paper would not have been written. We thank two anonymous referees, whose comments and criticisms resulted in an improved paper. We also thank A. Ferguson, C. Hoopes, and J. Rossa for access to high-quality versions of their figures as well as their permission to include them in this review. We are also very grateful to our students and collaborators for their support and contributions. R.J.R. thanks Don Cox for many valuable conversations over the years regard-

ing the nature of the WIM. R.J.R. and L.M.H. were supported by the National Science Foundation through Grants No. AST 02-04973 and No. AST 06-07512, with assistance from the University of Wisconsin's Graduate School, Department of Astronomy, and Department of Physics. G.J.M. acknowledges support from the University of Sydney Postdoctoral Fellowship Program and the National Science Foundation through Grant No. AST 04-01416. R.-J.D.'s work at Ruhr University-Bochum in this field is supported through DFG SFB 591 and through Deutsches Zentrum für Luft-und Raumfahrt through Grant No. 50 OR 9707. J.E.B., A.Z., and C.G. acknowledge support through Grant No. AYA2001-0435 from the Spanish Ministry of Science and Technology and Grant No. AYA2004-08251-C02-01 from the Ministry of Education and Science. A.Z. thanks the Consejería de Educación y Ciencia de la Junta de Andalucía, Spain, for support.

REFERENCES

- Alfaro, E. J., E. Pérez, and J. Franco, 2004, Eds., *How Does the Galaxy Work?* (Kluwer, Dordrecht).
- Ali, B., R. D. Blum, T. E. Bumgardner, S. R. Cranmer, G. J. Ferland, R. I. Haefner, and G. P. Tiede, 1991, "The [Ne III]-[O II] forbidden-line spectrum as an ionization indicator in nebulae," *Publ. Astron. Soc. Pac.* **103**, 1182–1186.
- Baker, R. I., L. M. Haffner, R. J. Reynolds, and G. J. Madsen, 2004, "WHAM multiwavelength observations of the ζ Oph H II region," *Bull. Am. Astron. Soc.* **36**, 1573.
- Beck, R., A. Brandenburg, D. Moss, A. Shukurov, and D. Sokoloff, 1996, "Galactic magnetism: Recent developments and perspectives," *Annu. Rev. Astron. Astrophys.* **34**, 155–206.
- Begelman, M. C., and A. C. Fabian, 1990, "Turbulent mixing layers in the interstellar and intracluster medium," *Mon. Not. R. Astron. Soc.* **244**, 26P–29P.
- Berkhuijsen, E. M., D. Mitra, and P. Mueller, 2006, "Filling factors and scale heights of the diffuse ionized gas in the Milky Way," *Astron. Nachr.* **327**, 82–96.
- Bland-Hawthorn, J., K. C. Freeman, and P. J. Quinn, 1997, "Where do the disks of spiral galaxies end?," *Astrophys. J.* **490**, 143–155.
- Bland-Hawthorn, J., and P. R. Maloney, 1999, "The escape of ionizing photons from the galaxy," *Astrophys. J. Lett.* **510**, L33–L36.
- Bland-Hawthorn, J., J. Sokolowski, and G. Cecil, 1991, "Imaging spectrophotometry of ionized gas in NGC 1068. II: Global ionization of the inner disk," *Astrophys. J.* **375**, 78–84.
- Bland-Hawthorn, J., R. Sutherland, O. Agertz, and B. Moore, 2007, "The source of ionization along the Magellanic Stream," *Astrophys. J. Lett.* **670**, L109–L112.
- Bloemen, J. B. G. M., E. R. Deul, and P. Thaddeus, 1990, "Decomposition of the FIR Milky Way observed by IRAS," *Astron. Astrophys.* **233**, 437–455.
- Boulares, A., and D. P. Cox, 1990, "Galactic hydrostatic equilibrium with magnetic tension and cosmic-ray diffusion," *Astrophys. J.* **365**, 544–558.
- Cecil, G., J. Bland-Hawthorn, and S. Veilleux, 2002, "Tightly correlated x-ray/H α -emitting filaments in the superbubble and large-scale superwind of NGC 3079," *Astrophys. J.* **576**, 745–752.
- Ciardi, B., S. Bianchi, and A. Ferrara, 2002, "Lyman continuum escape from an inhomogeneous interstellar medium," *Mon. Not. R. Astron. Soc.* **331**, 463–473.
- Clarke, C., and M. S. Oey, 2002, "Galactic porosity and a star formation threshold for the escape of ionizing radiation from galaxies," *Mon. Not. R. Astron. Soc.* **337**, 1299–1308.
- Collins, J. A., and R. J. Rand, 2001, "Ionization sources and physical conditions in the diffuse ionized gas halos of four edge-on galaxies," *Astrophys. J.* **551**, 57–71.
- Cowie, L. L., and C. F. McKee, 1977, "The evaporation of spherical clouds in a hot gas. I: Classical and saturated mass loss rates," *Astrophys. J.* **211**, 135–146.
- Cox, D. P., 2005, "The three-phase interstellar medium revisited," *Annu. Rev. Astron. Astrophys.* **43**, 337–385.
- Cox, D. P., and L. Helenius, 2003, "Flux-tube dynamics and a model for the origin of the local fluff," *Astrophys. J.* **583**, 205–228.
- Cox, D. P., and R. J. Reynolds, 1987, "The local interstellar medium," *Annu. Rev. Astron. Astrophys.* **25**, 303–344.
- Cox, P., and P. G. Mezger, 1989, "The Galactic infrared/submillimeter dust radiation," *Astron. Astrophys. Rev.* **1**, 49–83.
- Dahlem, M., U. Lisenfeld, and G. Golla, 1995, "Star formation activity in spiral galaxy disks and the properties of radio halos: Observational evidence for a direct dependence," *Astrophys. J.* **444**, 119–128.
- Dale, J. E., I. A. Bonnell, C. J. Clarke, and M. R. Bate, 2005, "Photoionizing feedback in star cluster formation," *Mon. Not. R. Astron. Soc.* **358**, 291–304.
- Davidson, K., and H. Netzer, 1979, "The emission lines of quasars and similar objects," *Rev. Mod. Phys.* **51**, 715–766.
- de Aveliz, M. A., and D. L. Berry, 2001, "Three-dimensional evolution of worms and chimneys in the Galactic disc," *Mon. Not. R. Astron. Soc.* **328**, 708–718.
- Dennison, B., J. H. Simonetti, and G. A. Topasna, 1998, "An imaging survey of northern Galactic H α emission with arcminute resolution," *Publ. Astron. Soc. Aust.* **15**, 147–148.
- Dettmar, R.-J., 1990, "The distribution of the diffuse ionized interstellar medium perpendicular to the disk of the edge-on galaxy NGC 891," *Astron. Astrophys.* **232**, L15–L18.
- Dettmar, R.-J., 1992, "Extraplanar diffuse ionized gas and the disk-halo connection in spiral galaxies," *Fundam. Cosmic Phys.* **15**, 143–208.
- Dettmar, R.-J., 1998, "Diffuse ionized gas in halos of spiral galaxies," in *IAU Colloquium 166: The Local Bubble and Beyond*, edited by D. Breitschwerdt, M. J. Freyberg, and J. Truemper, Lecture Notes in Physics Vol. 506 (Springer, Berlin), pp. 527–538.
- Dickey, J. M., and F. J. Lockman, 1990, "H I in the galaxy," *Annu. Rev. Astron. Astrophys.* **28**, 215–261.
- Domgorgen, H., and J. S. Mathis, 1994, "The ionization of the diffuse ionized gas," *Astrophys. J.* **428**, 647–653.
- Dopita, M. A., and R. S. Sutherland, 2003, *Astrophysics of the Diffuse Universe* (Springer, Berlin).
- Dove, J. B., and J. M. Shull, 1994, "Photoionization of the diffuse interstellar medium and galactic halo by OB associations," *Astrophys. J.* **430**, 222–235.
- Dove, J. B., J. M. Shull, and A. Ferrara, 2000, "The escape of ionizing photons from OB associations in disk galaxies: Radiation transfer through superbubbles," *Astrophys. J.* **531**, 846–860.
- Ellis, G. R. A., M. D. Waterworth, and M. S. Bessell, 1962,

- “Spectrum of the Galactic radio emission between 10 MHz and 1.5 MHz,” *Nature* **196**, 1079.
- Elmegreen, B. G., 1997, “Intercloud structure in a turbulent fractal interstellar medium,” *Astrophys. J.* **477**, 196–203.
- Elwert, T., 2005, private communication.
- Elwert, T., and R.-J. Dettmar, 2005, “Constraining the extra heating of the diffuse ionized gas in the Milky Way,” *Astrophys. J.* **632**, 277–282.
- Ercolano, B., M. J. Barlow, P. J. Storey, and X.-W. Liu, 2003, “MOCASSIN: A fully three-dimensional Monte Carlo photoionization code,” *Mon. Not. R. Astron. Soc.* **340**, 1136–1152.
- Ferguson, A. M. N., R. F. G. Wyse, J. S. Gallagher III, and D. A. Hunter, 1996, “Diffuse ionized gas in spiral galaxies: Probing Lyman continuum photon leakage from H II regions?,” *Astron. J.* **111**, 2265–2279.
- Ferland, G. J., 2001, “Physical conditions in the Orion H II region,” *Publ. Astron. Soc. Pac.* **113**, 41–48.
- Ferland, G. J., 2003, “Quantitative spectroscopy of photoionized clouds,” *Annu. Rev. Astron. Astrophys.* **41**, 517–554.
- Ferrière, K. M., 2001, “The interstellar environment of our galaxy,” *Rev. Mod. Phys.* **73**, 1031–1066.
- Field, G. B., 1975, “Heating and ionization of the interstellar medium—Star formation,” in *Atomic and Molecular Physics and the Interstellar Matter*, edited by R. Balian, P. Encrenaz, and J. Lequeux (North-Holland, Amsterdam), pp. 467–531.
- Finkbeiner, D. P., 2003, “A full-sky H α template for microwave foreground prediction,” *Astrophys. J., Suppl. Ser.* **146**, 407–415.
- Franco, J., G. Tenorio-Tagle, and P. Bodenheimer, 1990, “On the formation and expansion of H II regions,” *Astrophys. J.* **349**, 126–140.
- Frisch, P. C., and J. D. Slavin, 2003, “The chemical composition and gas-to-dust mass ratio of nearby interstellar matter,” *Astrophys. J.* **594**, 844–858.
- Gaensler, B. M., G. J. Madsen, S. Chatterjee, and S. A. Mao, 2008, “The vertical structure of warm ionised gas in the Milky Way,” *Publ. Astron. Soc. Aust.* **25**, 184–200.
- Gaustad, J. E., P. R. McCullough, W. Rosing, and D. Van Buren, 2001, “A robotic wide-angle H α survey of the southern sky,” *Publ. Astron. Soc. Pac.* **113**, 1326–1348.
- Giammanco, C., J. E. Beckman, and B. Cedrés, 2005, “Effects of photon escape on diagnostic diagrams for H II regions,” *Astron. Astrophys.* **438**, 599–610.
- Giammanco, C., J. E. Beckman, A. Zurita, and M. Relaño, 2004, “Propagation of ionizing radiation in H II regions: The effects of optically thick density fluctuations,” *Astron. Astrophys.* **424**, 877–885.
- Gry, C., and E. B. Jenkins, 2001, “Local clouds: Ionization, temperatures, electron densities and interfaces, from GHRS and IMAPS spectra of Epsilon Canis Majoris,” *Astron. Astrophys.* **367**, 617–628.
- Guélin, M., 1974, “Free electrons outside H II regions,” in *Galactic Radio Astronomy*, edited by F. J. Kerr and S. C. Simonson, Vol. 60 of IAU Symposium (Reidel, Dordrecht, The Netherlands), pp. 51–63.
- Haffner, L. M., 2005, “The ionized component of intermediate-velocity cloud complex L,” in *Extra-Planar Gas*, edited by R. Braun, Vol. 331 of Astronomical Society of the Pacific Conference Series (ASP, San Francisco), pp. 25–32.
- Haffner, L. M., R. J. Reynolds, and S. L. Tufte, 1999, “WHAM observations of H α , [S II], and [N II] toward the Orion and Perseus arms: Probing the physical conditions of the warm ionized medium,” *Astrophys. J.* **523**, 223–233.
- Haffner, L. M., R. J. Reynolds, and S. L. Tufte, 2001, “A map of the ionized component of the intermediate-velocity cloud complex K,” *Astrophys. J. Lett.* **556**, L33–L36.
- Haffner, L. M., R. J. Reynolds, S. L. Tufte, G. J. Madsen, K. P. Jaehnig, and J. W. Percival, 2003, “The Wisconsin H α Mapper Northern Sky Survey,” *Astrophys. J., Suppl. Ser.* **149**, 405–422.
- Hartmann, D., and W. B. Burton, 1997, *Atlas of Galactic Neutral Hydrogen* (Cambridge University Press, Cambridge, UK).
- Hausen, N. R., R. J. Reynolds, and L. M. Haffner, 2002, “Measurements of [O I] λ 6300/H α line intensity ratios for four O star H II regions,” *Astron. J.* **124**, 3336–3339.
- Heald, G. H., R. J. Rand, R. A. Benjamin, J. A. Collins, and J. Bland-Hawthorn, 2006, “Imaging Fabry-Perot spectroscopy of NGC 5775: Kinematics of the diffuse ionized gas halo,” *Astrophys. J.* **636**, 181–199.
- Heiles, C., 1986, “Supernovae, the interstellar medium, and the gaseous halo: The Swashbuckler’s approach,” in *Gaseous Halos of Galaxies*, edited by J. N. Bregman and F. J. Lockman (NRAO, Green Bank), p. 79.
- Hewish, A., S. J. Bell, J. D. Pilkington, P. F. Scott, and R. A. Collins, 1968, “Observation of a rapidly pulsating radio source,” *Nature* **217**, 709–713.
- Hidalgo-Gómez, A. M., 2005, “The diffuse ionized gas in the large telescopes era,” *Rev. Mex. Astron. Astros. Conf. Ser.* **24**, 288–293.
- Hill, A. S., R. A. Benjamin, G. Kowal, R. J. Reynolds, L. M. Haffner, and A. Lazarian, 2008, “The turbulent warm ionized medium: Emission measure distribution and MHD simulations,” *Astrophys. J.* **686**, 363–378.
- Hill, A. S., D. R. Stinebring, H. A. Barnor, D. E. Berwick, and A. B. Webber, 2003, “Pulsar scintillation arcs. I: Frequency dependence,” *Astrophys. J.* **599**, 457–464.
- Hills, J. G., 1972, “An explanation of the cloudy structure of the interstellar medium,” *Astron. Astrophys.* **17**, 155–160.
- Hoopes, C. G., and R. A. M. Walterbos, 2003, “Optical spectroscopy and ionization models of the diffuse ionized gas in M33, M51/NGC 5195, and M81,” *Astrophys. J.* **586**, 902–922.
- Howk, J. C., and B. D. Savage, 2000, “The multiphase halo of NGC 891: WIYN H α and BVI imaging,” *Astron. J.* **119**, 644–667.
- Howk, J. C., K. R. Sembach, and B. D. Savage, 2003, “Ionized gas in the first 10 kiloparsecs of the interstellar Galactic halo,” *Astrophys. J.* **586**, 249–267.
- Hoyle, F., and G. R. A. Ellis, 1963, “On the existence of an ionized layer about the Galactic plane,” *Aust. J. Phys.* **16**, 1–7.
- Kim, Y., G. H. Rieke, O. Krause, K. Misselt, R. Indebetouw, and K. E. Johnson, 2008, “Structure of the interstellar medium around Case A,” *Astrophys. J.* **678**, 287–296.
- Koo, B.-C., C. Heiles, and W. T. Reach, 1992, “Galactic worms. I: Catalog of worm candidates,” *Astrophys. J.* **390**, 108–132.
- Kowal, G., A. Lazarian, and A. Beresnyak, 2007, “Density fluctuations in MHD turbulence: Spectra, intermittency, and topology,” *Astrophys. J.* **658**, 423–445.
- Kulkarni, S. R., and C. Heiles, 1987, “The atomic component,” in *Interstellar Processes*, edited by D. J. Hollenbach and H. A. Thronson, Jr., Vol. 134 of Astrophysics and Space Science Library (Reidel, Dordrecht), pp. 87–122.
- Kutyrev, A. S., C. L. Bennett, S. H. Moseley, D. Rapchun, and K. P. Stewart, 2004, “Near Infrared Cryogenic Tunable Solid Fabry-Perot Spectrometer,” *Proc. SPIE* **5492**, 1172–1178.

- Lehnert, M. D., and T. M. Heckman, 1995, "Ionized gas in the halos of edge-on, starburst galaxies: Data and results," *Astrophys. J., Suppl. Ser.* **97**, 89–139.
- Lockman, F. J., 2004, "The hydrogen clouds in the Galactic halo," in *Recycling Intergalactic and Interstellar Matter*, edited by P.-A. Duc, J. Braine, and E. Brinks, Vol. 217 of IAU Symposium (ASP, San Francisco), p. 130.
- Mac Low, M.-M., and A. Ferrara, 1999, "Starburst-driven mass loss from dwarf galaxies: Efficiency and metal ejection," *Astrophys. J.* **513**, 142–155.
- Madsen, G. J., 2004, Ph.D. thesis (University of Wisconsin-Madison).
- Madsen, G. J., and R. J. Reynolds, 2005, "An investigation of diffuse interstellar gas toward a large, low-extinction window into the inner galaxy," *Astrophys. J.* **630**, 925–944.
- Madsen, G. J., R. J. Reynolds, and L. M. Haffner, 2006, "A multiwavelength optical emission line survey of warm ionized gas in the Galaxy," *Astrophys. J.* **652**, 401–425.
- Mathis, J. S., 1986, "The photoionization of the diffuse Galactic gas," *Astrophys. J.* **301**, 423–429.
- Mathis, J. S., 2000, "The warm ionized medium in the Milky Way and other galaxies," *Astrophys. J.* **544**, 347–355.
- Mathis, J. S., and K. Wood, 2005, "The effects of clumping on derived abundances in H II regions," *Mon. Not. R. Astron. Soc.* **360**, 227–235.
- McClure-Griffiths, N. M., A. Ford, D. J. Pisano, B. K. Gibson, L. Staveley-Smith, M. R. Calabretta, L. Dedes, and P. M. W. Kalberla, 2006, "Evidence for chimney breakout in the galactic supershell GSH 242–03+37," *Astrophys. J.* **638**, 196–205.
- McKee, C. F., and J. P. Ostriker, 1977, "A theory of the interstellar medium—Three components regulated by supernova explosions in an inhomogeneous substrate," *Astrophys. J.* **218**, 148–169.
- Mierkiewicz, E. J., R. J. Reynolds, F. L. Roesler, J. M. Harlander, and K. P. Jaehnig, 2006, "Detection of diffuse interstellar [O II] emission from the Milky Way using spatial heterodyne spectroscopy," *Astrophys. J. Lett.* **650**, L63–L66.
- Miller, S. T., and S. Veilleux, 2003, "Extraplanar emission-line gas in edge-on spiral galaxies. I: Deep emission-line imaging," *Astrophys. J., Suppl. Ser.* **148**, 383–417.
- Miller, W. W. I., and D. P. Cox, 1993, "The diffuse ionized interstellar medium: Structures resulting from ionization by O stars," *Astrophys. J.* **417**, 579–594.
- Minter, A. H., and S. R. Spangler, 1997, "Heating of the interstellar diffuse ionized gas via the dissipation of turbulence," *Astrophys. J.* **485**, 182–194.
- Monnet, G., 1971, "Evidence for a new class of very extended H II regions in the disks of Sc galaxies," *Astron. Astrophys.* **12**, 379–387.
- Norman, C. A., and S. Ikeuchi, 1989, "The disk-halo interaction—Superbubbles and the structure of the interstellar medium," *Astrophys. J.* **345**, 372–383.
- Och, S. R., L. B. Lucy, and M. R. Rosa, 1998, "Diffuse radiation in models of photoionized nebulae," *Astron. Astrophys.* **336**, 301–308.
- Oegerle, W. R., E. B. Jenkins, R. L. Shelton, D. V. Bowen, and P. Chayer, 2005, "A survey of O VI absorption in the local interstellar medium," *Astrophys. J.* **622**, 377–389.
- Oey, M. S., *et al.*, 2007, "The survey for ionization in neutral gas galaxies. III: Diffuse, warm ionized medium and escape of ionizing radiation," *Astrophys. J.* **661**, 801–814.
- Osterbrock, D., and E. Flather, 1959, "Electron densities in the Orion Nebula. II," *Astrophys. J.* **129**, 26–43.
- Osterbrock, D. E., 1989, *Astrophysics of Gaseous Nebulae and Active Galactic Nuclei* (University Science Books, Mill Valley).
- Osterbrock, D. E., and G. J. Ferland, 2006, *Astrophysics of Gaseous Nebulae and Active Galactic Nuclei* (University Science Books, Sausalito, CA).
- Otte, B., J. S. Gallagher III, and R. J. Reynolds, 2002, "Emission-line ratios and variations in temperature and ionization state in the diffuse ionized gas of five edge-on galaxies," *Astrophys. J.* **572**, 823–837.
- Otte, B., R. J. Reynolds, J. S. Gallagher III, and A. M. N. Ferguson, 2001, "Searching for additional heating: [O II] emission in the diffuse ionized gas of NGC 891, NGC 4631, and NGC 3079," *Astrophys. J.* **560**, 207–221.
- Pidopryhora, Y., F. J. Lockman, and J. C. Shields, 2007, "The Ophiuchus Superbubble: A gigantic eruption from the inner disk of the Milky Way," *Astrophys. J.* **656**, 928–942.
- Pildis, R. A., J. N. Bregman, and J. M. Schombert, 1994, "Extraplanar emission-line gas in edge-on galaxies," *Astrophys. J.* **427**, 160–164.
- Putman, M. E., J. Bland-Hawthorn, S. Veilleux, B. K. Gibson, K. C. Freeman, and P. R. Maloney, 2003, "H α emission from high-velocity clouds and their distances," *Astrophys. J.* **597**, 948–956.
- Ranalli, P., A. Comastri, and G. Setti, 2003, "The 2–10 keV luminosity as a star formation rate indicator," *Astron. Astrophys.* **399**, 39–50.
- Rand, R. J., 1996, "Diffuse ionized gas in nine edge-on galaxies," *Astrophys. J.* **462**, 712–724.
- Rand, R. J., 1997, "A very deep spectrum of the diffuse ionized gas in NGC 891," *Astrophys. J.* **474**, 129–139.
- Rand, R. J., 1998, "Further spectroscopy of the diffuse ionized gas in NGC 891 and evidence for a secondary source of ionization," *Astrophys. J.* **501**, 137–152.
- Rand, R. J., S. R. Kulkarni, and J. J. Hester, 1990, "The distribution of warm ionized gas in NGC 891," *Astrophys. J. Lett.* **352**, L1–L4.
- Raymond, J. C., 1992, "Microflare heating of the Galactic halo," *Astrophys. J.* **384**, 502–507.
- Reber, G., and G. R. Ellis, 1956, "Cosmic radio-frequency radiation near one megacycle," *J. Geophys. Res.* **61**, 1–10.
- Reynolds, R. J., 1971, Ph.D. thesis (University of Wisconsin-Madison).
- Reynolds, R. J., 1984, "A measurement of the hydrogen recombination rate in the diffuse interstellar medium," *Astrophys. J.* **282**, 191–196.
- Reynolds, R. J., 1985a, "Detection of the forbidden [O III] λ 5007 emission line in the Galactic background," *Astrophys. J.* **298**, L27–L30.
- Reynolds, R. J., 1985b, "[S II] λ 6716 in the Galactic emission-line background," *Astrophys. J.* **294**, 256–262.
- Reynolds, R. J., 1988, "[S II]/H α intensity ratios in faint, extended H II regions and the origin of the interstellar emission-line background," *Astrophys. J.* **333**, 341–352.
- Reynolds, R. J., 1989, "The column density and scale height of free electrons in the Galactic disk," *Astrophys. J. Lett.* **339**, L29–L32.
- Reynolds, R. J., 1991a, "Ionized disk/halo gas—insight from optical emission lines and pulsar dispersion measures," in *The Interstellar Disk-Halo Connection in Galaxies*, edited by H. Bloemen, Vol. 144 of IAU Symposium (Kluwer, Dordrecht), pp. 67–76.
- Reynolds, R. J., 1991b, "Line integrals of n_e and n_e^2 at high

- Galactic latitude," *Astrophys. J. Lett.* **372**, L17–L20.
- Reynolds, R. J., 2004, "Warm ionized gas in the local interstellar medium," *Adv. Space Res.* **34**, 27–34.
- Reynolds, R. J., V. Chaudhary, G. J. Madsen, and L. M. Haffner, 2005, "Unresolved H α enhancements at high galactic latitude in the WHAM sky survey maps," *Astron. J.* **129**, 927–934.
- Reynolds, R. J., and D. P. Cox, 1992, "Heating the warm ionized medium," *Astrophys. J. Lett.* **400**, L33–L34.
- Reynolds, R. J., L. M. Haffner, and S. L. Tufte, 1999, "Evidence for an additional heat source in the warm ionized medium of galaxies," *Astrophys. J. Lett.* **525**, L21–L24.
- Reynolds, R. J., N. R. Hausen, S. L. Tufte, and L. M. Haffner, 1998, "Detection of [O I] λ 6300 emission from the diffuse interstellar medium," *Astrophys. J. Lett.* **494**, L99–L102.
- Reynolds, R. J., and P. M. Ogden, 1979, "Optical evidence for a very large, expanding shell associated with the I Orion OB Association, Barnard's Loop, and the high Galactic latitude H α filaments in Eridanus," *Astrophys. J.* **229**, 942–953.
- Reynolds, R. J., F. Scherb, and F. L. Roesler, 1973, "Observations of diffuse Galactic H α and [N II] emission," *Astrophys. J.* **185**, 869–876.
- Reynolds, R. J., N. C. Sterling, and L. M. Haffner, 2001, "Detection of a large arc of ionized hydrogen far above the casiopeia OB6 Association: A superbubble blowout into the Galactic halo?," *Astrophys. J. Lett.* **558**, L101–L104.
- Reynolds, R. J., N. C. Sterling, L. M. Haffner, and S. L. Tufte, 2001, "Detection of [N II] λ 5755 emission from low-density ionized interstellar gas," *Astrophys. J. Lett.* **548**, L221–L224.
- Reynolds, R. J., and S. L. Tufte, 1995, "A search for the He I λ 5876 recombination line from the diffuse interstellar medium," *Astrophys. J. Lett.* **439**, L17–L20.
- Reynolds, R. J., S. L. Tufte, D. T. Kung, P. R. McCullough, and C. Heiles, 1995, "A comparison of diffuse ionized and neutral hydrogen away from the Galactic plane: H α -emitting H I clouds," *Astrophys. J.* **448**, 715–726.
- Ricotti, M., and J. M. Shull, 2000, "Feedback from galaxy formation: Escaping ionizing radiation from galaxies at high redshift," *Astrophys. J.* **542**, 548–558.
- Rossa, J., and R.-J. Dettmar, 2000, "Extraplanar diffuse ionized gas in a small sample of nearby edge-on galaxies," *Astron. Astrophys.* **359**, 433–446.
- Rossa, J., and R.-J. Dettmar, 2003a, "An H α survey aiming at the detection of extraplanar diffuse ionized gas in halos of edge-on spiral galaxies. I. How common are gaseous halos among non-starburst galaxies?," *Astron. Astrophys.* **406**, 493–503.
- Rossa, J., and R.-J. Dettmar, 2003b, "An H α survey aiming at the detection of extraplanar diffuse ionized gas in halos of edge-on spiral galaxies. II. The H α survey atlas and catalog," *Astron. Astrophys.* **406**, 505–525.
- Rossa, J., R.-J. Dettmar, R. A. M. Walterbos, and C. A. Norman, 2004, "A Hubble Space Telescope WFPC2 investigation of the disk-halo interface in NGC 891," *Astron. J.* **128**, 674–686.
- Rozas, M., A. Zurita, C. H. Heller, and J. E. Beckman, 1999, "Global properties of the population of H II regions in NGC 7479 from photometric H α imaging," *Astron. Astrophys. Suppl. Ser.* **135**, 145–158.
- Savage, B. D., K. R. Sembach, B. P. Wakker, P. Richter, M. Meade, E. B. Jenkins, J. M. Shull, H. W. Moos, and G. Sonneborn, 2003, "Distribution and kinematics of O VI in the Galactic halo," *Astrophys. J., Suppl. Ser.* **146**, 125–164.
- Savage, B. D., *et al.*, 2000, "Far ultraviolet spectroscopic explorer observations of O VI absorption in the Galactic halo," *Astrophys. J. Lett.* **538**, L27–L30.
- Sembach, K. R., J. C. Howk, R. S. I. Ryans, and F. P. Keenan, 2000, "Modeling the warm ionized interstellar medium and its impact on elemental abundance studies," *Astrophys. J.* **528**, 310–324.
- Sembach, K. R., and B. D. Savage, 1992, "Observations of highly ionized gas in the Galactic halo," *Astrophys. J., Suppl. Ser.* **83**, 147–201.
- Sembach, K. R., B. P. Wakker, B. D. Savage, P. Richter, M. Meade, J. M. Shull, E. B. Jenkins, G. Sonneborn, and H. W. Moos, 2003, "Highly ionized high-velocity gas in the vicinity of the galaxy," *Astrophys. J., Suppl. Ser.* **146**, 165–208.
- Shapiro, P. R., and R. A. Benjamin, 1991, "New results concerning the Galactic fountain," *Publ. Astron. Soc. Pac.* **103**, 923–927.
- Slavin, J. D., and P. C. Frisch, 2002, "The ionization of nearby interstellar gas," *Astrophys. J.* **565**, 364–379.
- Slavin, J. D., J. M. Shull, and M. C. Begelman, 1993, "Turbulent mixing layers in the interstellar medium of galaxies," *Astrophys. J.* **407**, 83–99.
- Smith, R. K., *et al.*, 2007, "Suzaku observations of the local and distant hot ISM," *Pub. Astron. Soc. Jpn.* **59**, 141–150.
- Spitzer, L., 1978, *Physical Processes in the Interstellar Medium* (Wiley-Interscience, New York).
- Spitzer, L. J., and E. L. Fitzpatrick, 1993, "Composition of interstellar clouds in the disk and halo. I: HD 93521," *Astrophys. J.* **409**, 299–318.
- Strickland, D. K., T. M. Heckman, E. J. M. Colbert, C. G. Hoopes, and K. A. Weaver, 2004a, "A high spatial resolution x-ray and H α study of hot gas in the halos of star-forming disk galaxies. I: Spatial and spectral properties of the diffuse x-ray emission," *Astrophys. J., Suppl. Ser.* **151**, 193–236.
- Strickland, D. K., T. M. Heckman, E. J. M. Colbert, C. G. Hoopes, and K. A. Weaver, 2004b, "A high spatial resolution x-ray and H α study of hot gas in the halos of star-forming disk galaxies. II: Quantifying supernova feedback," *Astrophys. J.* **606**, 829–852.
- Strömgren, B., 1939, "The physical state of interstellar hydrogen," *Astrophys. J.* **89**, 526–547.
- Strömgren, B., 1948, "On the density distribution and chemical composition of the interstellar gas," *Astrophys. J.* **108**, 242–275.
- Terebey, S., M. Fich, R. Taylor, Y. Cao, and T. Hancock, 2003, "The impact of ionizing stars on the diffuse interstellar medium: A swept-up shell and ionized halo around the W4 chimney/superbubble," *Astrophys. J.* **590**, 906–916.
- Tufte, S. L., 1997, Ph.D. thesis (University of Wisconsin-Madison).
- Tufte, S. L., R. J. Reynolds, and L. M. Haffner, 1998, "WHAM observations of H α emission from high-velocity clouds in the M, A, and C complexes," *Astrophys. J.* **504**, 773–784.
- Tufte, S. L., J. D. Wilson, G. J. Madsen, L. M. Haffner, and R. J. Reynolds, 2002, "WHAM observations of H α from high-velocity clouds: Are they Galactic or extragalactic?," *Astrophys. J. Lett.* **572**, L153–L156.
- Tüllmann, R., and R.-J. Dettmar, 2000, "Spectroscopy of diffuse ionized gas in halos of selected edge-on galaxies," *Astron. Astrophys.* **362**, 119–132.
- Tüllmann, R., R.-J. Dettmar, M. Soida, M. Urbanik, and J. Rossa, 2000, "The thermal and non-thermal gaseous halo of NGC 5775," *Astron. Astrophys.* **364**, L36–L41.

- Tüllmann, R., W. Pietsch, J. Rossa, D. Breitschwerdt, and R.-J. Dettmar, 2006, "The multi-phase gaseous halos of star forming late-type galaxies. I: XMM-Newton observations of the hot ionized medium," *Astron. Astrophys.* **448**, 43–75.
- Veilleux, S., G. Cecil, and J. Bland-Hawthorn, 2005, "Galactic winds," *Annu. Rev. Astron. Astrophys.* **43**, 769–826.
- Voges, E. S., 2006, Ph.D. thesis (New Mexico State University).
- Voges, E. S., and R. A. M. Walterbos, 2006, "Detection of [O I] λ 6300 and other diagnostic emission lines in the diffuse ionized gas of M33 with Gemini-North," *Astrophys. J. Lett.* **644**, L29–L32.
- Wakker, B. P., 2004, "Recent developments concerning high-velocity clouds," *Astrophys. Space Sci.* **289**, 381–390.
- Wang, Q. D., S. Immler, R. Walterbos, J. T. Lauroesch, and D. Breitschwerdt, 2001, "Chandra detection of a hot gaseous corona around the edge-on galaxy NGC 4631," *Astrophys. J. Lett.* **555**, L99–L102.
- Weiner, B. J., and T. B. Williams, 1996, "Detection of H α emission from the Magellanic Stream: Evidence for an extended gaseous Galactic halo," *Astron. J.* **111**, 1156–1163.
- Weingartner, J. C., and B. T. Draine, 2001, "Photoelectric emission from interstellar dust: Grain charging and gas heating," *Astrophys. J., Suppl. Ser.* **134**, 263–281.
- Williams, R. E., 1992, "Incorporation of density fluctuations into photoionization calculations," *Astrophys. J.* **392**, 99–105.
- Wood, K., L. M. Haffner, R. J. Reynolds, J. S. Mathis, and G. Madsen, 2005, "Estimating the porosity of the interstellar medium from three-dimensional photoionization modeling of H II regions," *Astrophys. J.* **633**, 295–308.
- Wood, K., and A. Loeb, 2000, "Escape of ionizing radiation from high-redshift galaxies," *Astrophys. J.* **545**, 86–99.
- Wood, K., and J. S. Mathis, 2004, "Monte carlo photoionization simulations of diffuse ionized gas," *Mon. Not. R. Astron. Soc.* **353**, 1126–1134.
- Wood, K., J. S. Mathis, and B. Ercolano, 2004, "A three-dimensional Monte Carlo photoionization code for modelling diffuse ionized gas," *Mon. Not. R. Astron. Soc.* **348**, 1337–1347.
- Zurita, A., J. E. Beckman, M. Rozas, and S. Ryder, 2002, "The origin of the ionization of the diffuse ionized gas in spirals. II: Modelling the distribution of ionizing radiation in NGC 157," *Astron. Astrophys.* **386**, 801–815.
- Zurita, A., M. Rozas, and J. E. Beckman, 2000, "The origin of the ionization of the diffuse interstellar medium in spiral galaxies. I: Photometric measurements," *Astron. Astrophys.* **363**, 9–28.